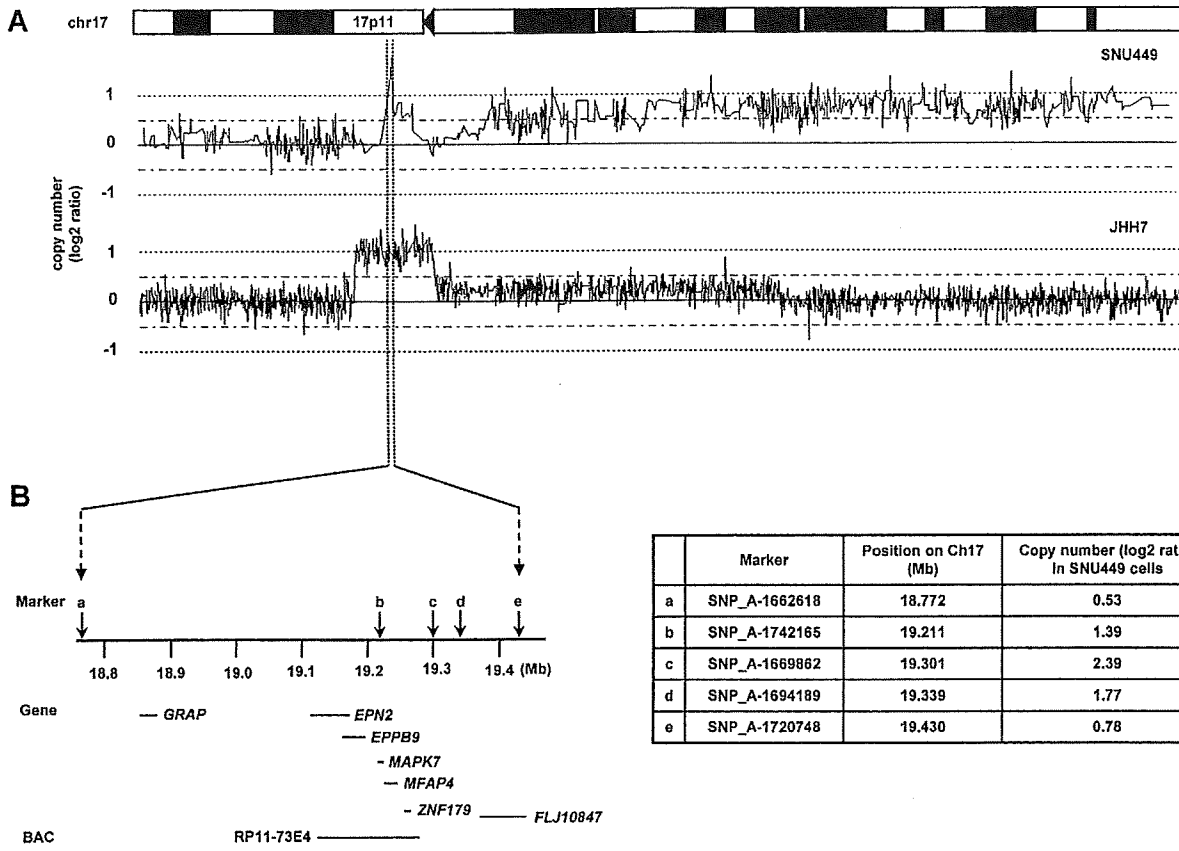

	Marker	Position on Ch17 (Mb)	Copy number (log2 ratio) in SNU449 cells
a	SNP_A-1662618	18.772	0.53
b	SNP_A-1742165	19.211	1.39
c	SNP_A-1669862	19.301	2.39
d	SNP_A-1694189	19.339	1.77
e	SNP_A-1720748	19.430	0.78

Figure 1. Map of the amplicon at 17p11 in two HCC cell lines. A: Copy number profiles for chromosome 17 in SNU449 and JHH-7 cells. Copy number values were determined by SNP 100K and 250K array analyses for SNU449 and JHH-7 cells, respectively. B: The smallest common region of amplification in SNU449 and JHH-7 cells (left). The position of the Affymetrix SNP markers, the seven genes within the amplicon (*GRAP*, *EPN2*, *EPPB9*, *MAPK7*, *MFAP4*, *ZNF179*, and *FLJ10847*) and the BAC RP11-73E4 (used as a probe for FISH) are numbered according to the UCSC genome database (http://genome.ucsc.edu/). Detailed copy-number information at positions identified by individual SNP markers over the amplified region in SNU449 cells is shown at right.

these experiments was BAC RP11-73E4, which contains *EPN2*, *EPPB9*, *MAPK7*, *MFAP4*, and *ZNF179* (Fig. 1B). This probe showed an amplified FISH signal on metaphase chromosomes from SNU449 cells (Fig. 2A). To further characterize the relationship between the genes in this chromosomal region and amplifications observed in cancer cells, we analyzed the gene dosage of the *MAPK7* locus by real-time quantitative PCR of DNA from 21 different liver cancer cell lines (20 HCC cell lines and the hepatoblastoma line HepG2). Amplification of *MAPK7* was observed in SNU449 and JHH-7 cells (Fig. 2B). Taken together, the data provide strong evidence that the 17p11 region is amplified in SNU449 and JHH-7 cells.

Analysis of Positional Candidate Genes in HCC Cell Lines

The 17p11 region may harbor one or more genes (henceforth referred to as "target genes") that, when activated by amplification, play a role in carcinogenesis. A common criterion for designating a gene as a putative target is that amplification leads to its overexpression (Collins et al., 1998). Thus, using real-time quantitative PCR, we determined the mRNA levels of all seven genes in the 17p11 amplicon in our panel of 21 liver cancer cell lines. As shown in Fig. 2C, the *EPN2*, *EPPB9*, and *MAPK7* genes were overexpressed in both SNU449 and JHH-7 cells. In several other lines, one or more of these three genes was overexpressed, despite the fact that regional amplification was not observed. These findings suggest that *EPN2*, *EPPB9*, and *MAPK7* are candidate target genes for 17p11 amplification.

Of these three genes, we chose to focus further analysis on *MAPK7*, which encodes ERK5, because ERK5-related proteins have been previously implicated in carcinogenesis (Hayashi and Lee, 2004; Wang and Tournier, 2006), whereas there is little or no evidence linking *EPN2* or

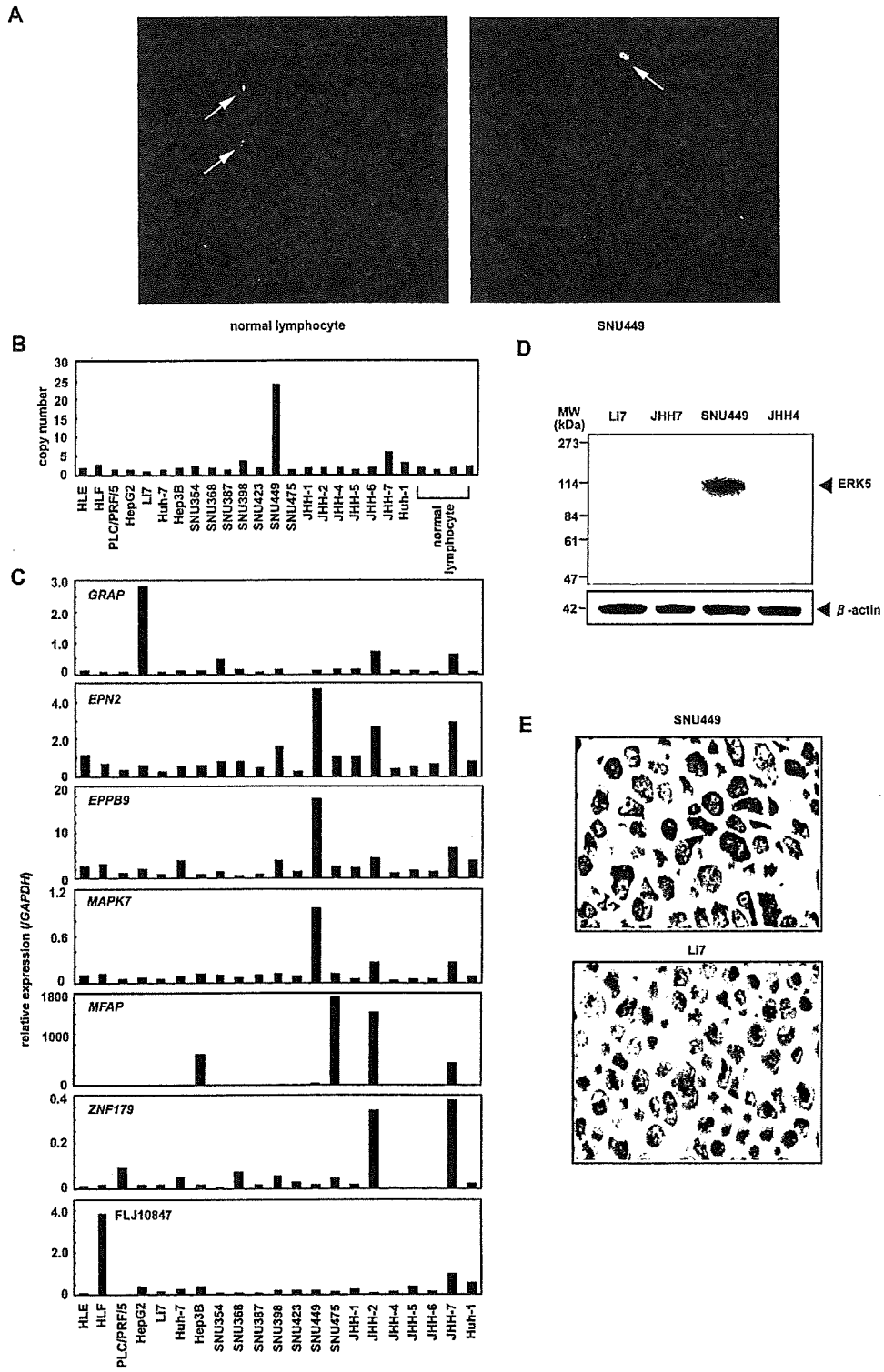

Figure 2. Amplification and overexpression of *MAPK7* in HCC cell lines. (A) Representative images from FISH analysis using a BAC RP11-73E4 probe on metaphase chromosomes from normal lymphocytes and SNU449 cells. While the probe shows a normal signal pattern (2 copies/cell) in normal lymphocytes (arrows, left), it shows an amplified signal in SNU449 cells (arrow, right). (B) Copy number of *MAPK7* in 21 liver cancer cell lines (20 HCC cells and one hepatoblastoma line, HepG2) and four peripheral blood lymphocytes (normal cell controls) as measured by real-time quantitative PCR with reference to a LINE-1 control. Values were normalized such that the average copy number of *MAPK7* in genomic DNA derived from normal lymphocytes is 2. (C) Relative expression levels of the seven genes within the 17p11 amplicon in a panel of 21 liver cancer cell lines as determined by real-time quantitative RT-PCR. The results are presented as the ratio between the expression level of each gene and a reference gene (*GAPDH*) to correct for variation in the amount of RNA. (D) Immunoblot analysis to detect protein levels of ERK5 and β-actin, an internal control, in four HCC cell lines with different *MAPK7* DNA copy numbers (B) and mRNA levels (C). (E) Immunostaining of ERK5 in SNU449 and LI7 cells.

EPPB9 to tumorigenesis. Immunoblot analysis revealed that ERK5 expression is upregulated in SNU449 cells. Indeed, among the HCC cell lines that were tested, SNU449 showed the highest level of both 17p11 amplification and *MAPK7* overexpression (Fig. 2D). Moreover, immunostaining confirmed that the level of ERK5 was elevated in SNU449 cells. ERK5 was strongly expressed in the cytoplasm of SNU449 cells (Fig. 2E). In contrast, ERK5 was weakly expressed in only a few Li7 cells, a HCC cell line that shows neither amplification nor overexpression of *MAPK7* (Fig. 2E).

Copy Number Gain of *MAPK7* in Primary HCC Tumors

To determine whether *MAPK7* is amplified in primary tumors, we examined 66 primary HCCs for copy number gains using real-time quantitative PCR. Copy number changes were counted as gains if the results of the analysis for a given tumor cell type exceeded the mean plus twice the standard deviation (SD) of the levels of *MAPK7* observed in genomic DNA derived from four peripheral blood lymphocyte samples (i.e., normal cells). A copy number gain for *MAPK7* was observed in 35 of the 66 tumors (53%; Fig. 3).

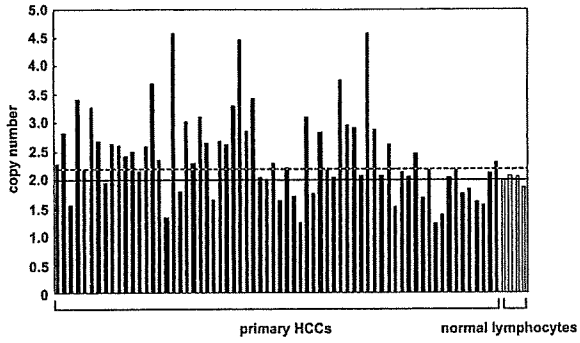

Figure 3. Copy number gain of *MAPK7* in primary HCC tumors. Copy numbers of *MAPK7* in 66 primary HCC tumors and four normal peripheral blood lymphocytes were determined by real-time quantitative PCR with reference to a LINE-1 control. Values were normalized such that the average copy number of *MAPK7* in genomic DNA derived from the normal lymphocytes equals 2 (solid horizontal line). The mean + 2 × SD of normal lymphocytes was used as the cutoff value for copy number gain (dotted line).

Expression of ERK5 in Primary HCCs

We next examined the level of ERK5 in 43 additional primary HCCs, including paired tumor and surrounding nontumor tissues. Immunohistochemical studies revealed that, in nontumor tissues (normal liver, chronic hepatitis, or liver cirrhosis), ERK5 is strongly expressed in bile ducts, bile ductules, and a few small hepatocytes (Fig. 4A). In these cells, ERK5 was present in the cytoplasm. Hepatocytes also contained ERK5, although at a lower level than in bile ducts (Fig. 4A). The staining pattern for ERK5 was almost identical for normal liver, chronic hepatitis, and liver cirrhosis.

This granular cytoplasmic staining for ERK5 was also observed in HCC cancer cells (Fig. 4B). HCC cells containing ERK5 were uniformly distributed in the tumor tissues. The level of ERK5 was elevated in 11 of the 43 tumors compared with the paired nontumor tissues (Figs. 4B and 4C; Supp. Info. Table 1). To clarify the relationship between the level of ERK5 and various clinicopathological parameters, we examined available data from the 43 patients, whose tumors were divided into elevated (T>NT) and not elevated (T≤NT) groups. There was no significant correlation between the level of ERK5 and any parameter examined, including age and gender of the patients; size, stage, and degree of differentiation of the tumor; HBV or HCV infection; and

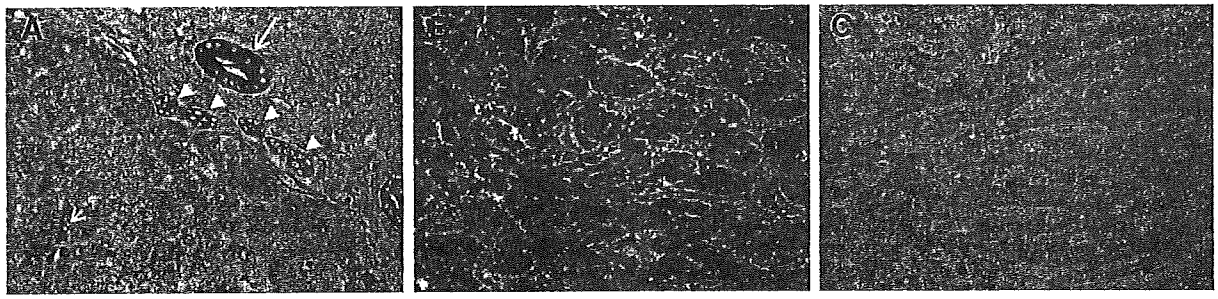

Figure 4. Representative ERK5 immunostaining of tissues. (A) A nontumorous liver tissue (chronic hepatitis). The level of ERK5 is elevated in the bile duct (large arrow), bile ductules (arrowheads), and a few small hepatocytes (small arrow). (B, C) Paired tumor (B) and nontumor (C) tissues from one HCC patient, wherein the level of ERK5 is elevated in the tumor compared with the counterpart nontumor tissue. Original magnification, ×400.

features of nontumorous liver tissues (Supp. Info. Table 1).

Downregulation of *MAPK7* Inhibits the Growth of HCC Cells

To investigate the effects of *MAPK7* overexpression on HCC cells, we knocked down its expression using RNAi. In SNU449 cells treated with siRNA targeting *MAPK7*, we observed a decrease in *MAPK7* mRNA and ERK5 protein levels relative to that observed for cells receiving a control siRNA or transfection agent alone (Figs. 5A and 5B). The siRNA-mediated downregulation of *MAPK7* suppressed the growth of SNU449 cells at all time points assayed over a 72-hr period (Fig. 5C). These findings suggest that ERK5 promotes the growth of HCC cells.

ERK5 is Phosphorylated During the G2/M Phases of the Cell Cycle

To help elucidate the underlying mechanism by which ERK5 regulates cellular proliferation we investigated the role of ERK5 in cell cycle progression. SNU449 cells were synchronized at G1/S, early S, or M phases of the cell cycle using a double-thymidine, aphidicolin, or nocodazole block, respectively. We determined the levels of total ERK5 and phosphorylated (active) form of ERK5. Immunoblotting did not show a difference in the level of total ERK5 among the three phases of the cell cycle (Fig. 6A). To detect phosphorylated ERK5, total ERK5 was immunoprecipitated from cell lysates using an anti-ERK5 antibody and then analyzed by immunoblotting using an anti-phospho-ERK5 antibody. Phosphorylated ERK5 was more abundant in cells synchronized at the M phase than in asynchronous cells (Fig. 6B).

We next synchronized SNU449 cells at the G1/S boundary using a double-thymidine block and then released the cells from the block. Using flow cytometry, we confirmed the synchrony of the cell cycle and monitored its progression after removal of thymidine (Fig. 6C). There was no difference in the level of total ERK5 during progression of the cell cycle (Fig. 6D). Expression of phosphorylated ERK was maximal 9 hr after release from the block (Fig. 6E), a time when a large proportion of cells were in the G2/M phase (Fig. 6C). Taken together, these observations indicate that ERK5 is phosphorylated during the G2/M phases of the cell cycle.

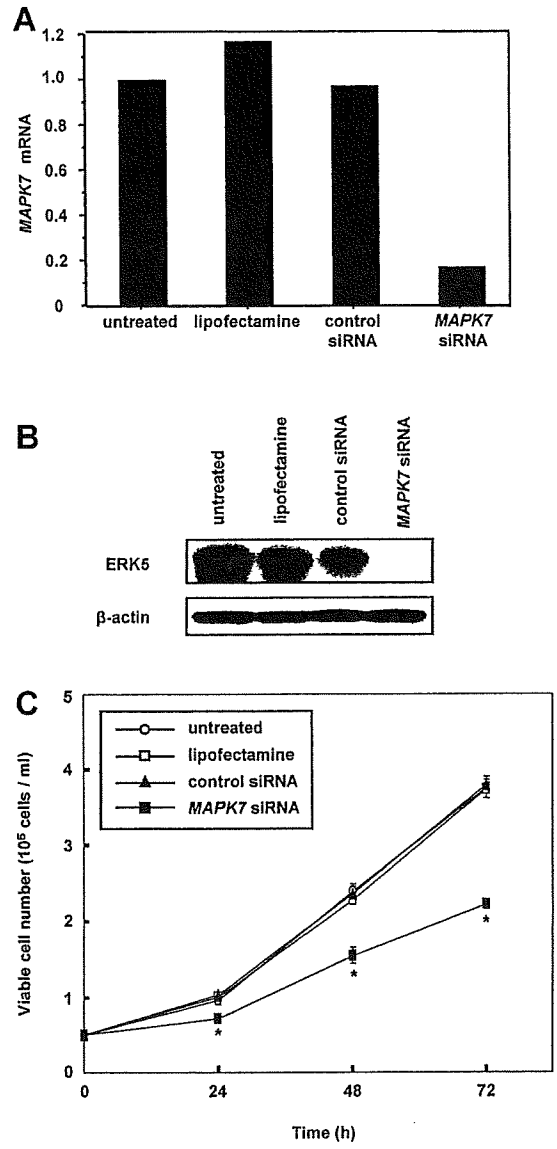

Figure 5. Growth inhibition of SNU449 cells by knockdown of *MAPK7*. A: Relative expression levels of *MAPK7* mRNA as determined by real-time quantitative RT-PCR. SNU449 cells were treated with siRNA targeting *MAPK7*, negative control siRNA, or the transfection agent alone (Lipofectamine), and harvested 48 hr after transfection. Untreated cells were maintained under identical experimental conditions. Results are presented as a ratio between the expression level of *MAPK7* and that of a reference gene (*GAPDH*) to correct for variation in the amount of RNA. Relative expression levels were normalized such that the ratio in untreated cells is 1. B: Levels of ERK5 and β-actin, an internal control, determined by immunoblotting. C: Cell growth was assayed by counting the viable cells at the indicated times after transfection. Each assay was performed in triplicate. Values are represented as the mean ± SD. Differences were analyzed by ANOVA (*$P < 0.01$).

ERK5 Regulates Entry into Mitosis

Our results indicating that ERK5 is activated during the G2/M phases in SNU449 cells suggested that ERK5 may be involved in G2/M progression. To examine whether ERK5 plays a role in mitotic entry, we knocked down *MAPK7*

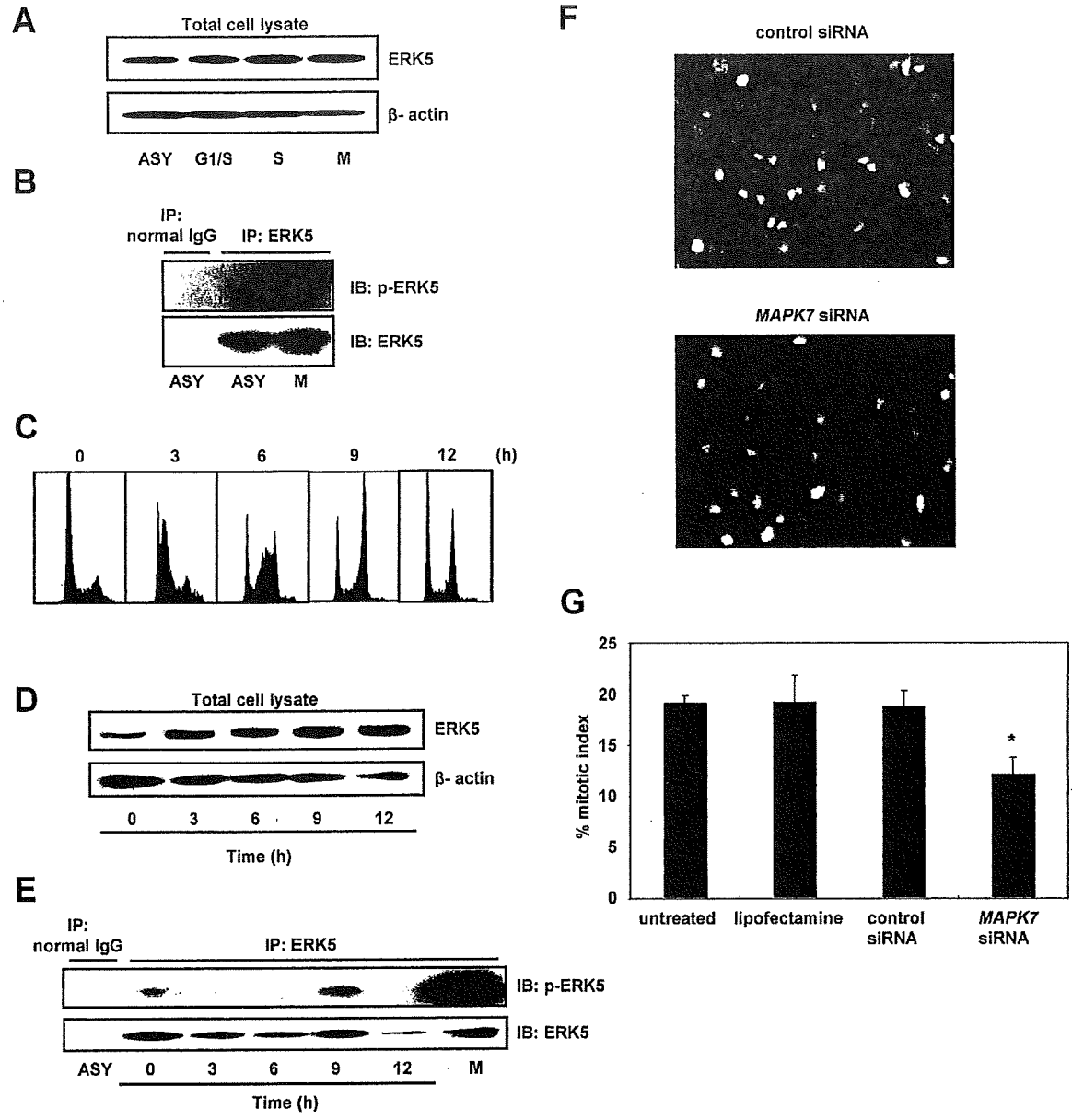

Figure 6. ERK5 is phosphorylated during the G2/M phases of the cell cycle. (A) Immunoblot analysis to detect protein levels of total ERK5 and β-actin, an internal control, in SNU449 cells that were synchronized at the G1/S, early S, or M phases using a double-thymidine, aphidicolin, or nocodazole block, respectively, or were untreated and used as an asynchronous (ASY) population. (B) Levels of phosphorylated ERK5 (p-ERK5). ERK5 was immunoprecipitated (IP) from lysates of SNU449 cells that were synchronized at the M phase (M) or from asynchronous cells (ASY). The samples were split and analyzed by immunoblotting (IB) for p-ERK5 and total ERK5. Normal rabbit immunoglobulin (normal IgG) was used as a negative control for immunoprecipitation. (C) Flow cytometric analysis. SNU449 cells were synchronized to the G1/S boundary using a double-thymidine block. Synchronized cells were released from the block and harvested at the indicated time points. The X-axis indicates DNA content and the Y-axis indicates the number of cells. (D) Time course of changes in the level of total ERK5 after release from the double-thymidine block. The level of β-actin was used as an internal control. (E) Time course of changes in the level of p-ERK5 after release from the double-thymidine block. ERK5 was immunoprecipitated from lysates of SNU449 cells harvested at the indicated times after release from the double-thymidine block. The samples were split and analyzed by immunoblotting for p-ERK5 and total ERK5. SNU449 cells, synchronized at the M phase with nocodazole, were also examined as described in (A) and (B). Normal rabbit IgG was used as a negative control for immunoprecipitation. (F) Representative images of mitotic cells in an SNU449 cell population that was transfected with *MAPK7*- or control-siRNA. SNU449 cells were treated with siRNA targeting *MAPK7*, negative control siRNA, or the transfection agent alone (Lipofectamine). Untreated cell were maintained under identical conditions. These cells were synchronized at the G1/S boundary using a double-thymidine block. The synchronized cells were released from the block and stained with anti-phospho-histone H3 9 hr after release, a time corresponding to the G2/M phase as shown in (C). Mitotic cells were identified by positive staining for phospho-histone H3 (green). Nuclear DNA was stained with propidium iodide (red). (G) The mitotic index was scored as described in Materials and Methods section. Data are presented as means ± SD (ANOVA; $*P < 0.05$).

expression using RNAi and assessed its effect on mitosis. SNU449 cells were transfected with siRNA targeting *MAPK7* and synchronized at the G1/S-phase boundary by a double-thymidine block. The synchronized cells were released from the block and harvested 9 hr after release, a time which corresponds to the G2/M phase (Fig. 6C). Finally, harvested cells were stained with anti-phospho-histone H3 antibody, which specifically detects mitotic cells (Fig. 6F). Compared with a control siRNA or transfection agent alone, transfection of *MAPK7* siRNA significantly reduced the mitotic index (Fig. 6G). These findings suggest that ERK5 regulates mitotic entry in the HCC cells.

DISCUSSION

High-density SNP arrays are powerful tools for high-resolution analysis of DNA copy number aberrations in cancers. In the present study, using the Affymetrix GeneChip 100K and 250K SNP arrays we detected a novel amplification in HCC cells at 17p11. We were able to narrow the amplification to a 750-kb region. Notably, the amplification might have been missed using conventional analyses such as CGH. Amplification at 17p11.2-p12 has been detected in high-grade osteosarcoma using CGH (Forus et al., 1995; Tarkkanen et al., 1995). The group of van Dartel et al., (2002) established 17p11.2-p12 amplification profiles by semi-quantitative PCR using 15 microsatellite markers and seven candidate genes to assay amplification in this tumor type. They found that most of the tumors had complex amplification profiles, suggesting that multiple amplification targets, including *MAPK7*, might be present in region 17p11.2-p12. In contrast, we were able to define a smaller common region of amplification at 17p11 in two HCC cells and to determine the expression status of all genes in the amplicon. Three of the seven genes in the amplicon; *EPN2*, *EPPB9*, and *MAPK7*, were always overexpressed in cells that showed amplification in the 17p11 region. Thus, we considered these three genes as candidate targets for amplification. The function of *EPPB9* (B9 protein) is not known, and the protein encoded by *EPN2* (epsin 2) is similar to epsin 1, which plays a putative role in clathrin-mediated endocytosis (Rosenthal et al., 1999). Therefore, we focused on *MAPK7* as a target for the amplification.

Several lines of evidence implicate ERK5, which is encoded by *MAPK7*, in tumorigenesis (Wang and Tournier, 2006): (a) the ERK5 pathway is activated by Ras (English et al., 1999), ErbB (Esparis-Ogando et al., 2002; Yuste et al., 2005), Src (Sun et al., 2003), Cot (Chiariello et al., 2000), Bcr-Abl (Buschbeck et al., 2005), insulin-like growth factor-II (Linnerth et al., 2005), and interleukin-6 (Carvajal-Vergara et al., 2005); (b) ERK5 is involved in the control of breast cancer cell proliferation (Esparis-Ogando et al., 2002); (c) ERK5 mediates a survival signal that confers chemoresistance to breast cancer (Weldon et al., 2002); (d) insulin-like growth factor-II promotes cell survival via the ERK5 pathway in lung cancer cells (Linnerth et al., 2005); (e) the level of ERK5 contributes to the survival of Bcr/Abl-positive leukemic cells (Buschbeck et al., 2005); (f) ERK5 regulates cell proliferation and antiapoptotic responses in multiple myeloma (Carvajal-Vergara et al., 2005); and (g) an elevated level of MEK5, a specific activator of ERK5, is associated with metastasis and a poor prognosis in prostate cancer (Mehta et al., 2003).

The present study is the first to show the status of amplification and expression of *MAPK7* and its functional role in HCC. We found that *MAPK7* is amplified in 35 of 66 HCC tumors (53%). However, we could not determine the copy number of *MAPK7* in the nontumorous counterparts of the samples assayed because these samples were not available. Therefore, we cannot exclude the possibility that copy number polymorphism might influence the results of copy number analysis. We studied the expression of ERK5 using immunohistochemical analysis in primary HCCs and their surrounding nontumorous liver tissues. In nontumorous liver tissues, ERK5 was weakly expressed in the cytoplasm of non-neoplastic hepatocytes. Intriguingly, it was more strongly expressed in bile ducts, bile ductules, and a few small hepatocytes. In HCC tumor tissues, ERK5 was expressed in the cytoplasm of tumor cells. The level of ERK5 was elevated in 11 of 43 HCC tumors compared with their nontumorous counterparts. However, we did not observe a significant link between the level of ERK5 and any clinicopathological parameters. A recent report showed that, in prostate cancer, an increase in ERK5 cytoplasmic signals correlates with advanced disease and that strong nuclear ERK5 localization correlates with poor survival (McCracken et al., 2008).

We examined the functional roles of ERK5 in HCC cells using RNAi. Downregulation of *MAPK7* by siRNA suppressed the growth of

SNU449 cells, which had the greatest amplification and overexpression of *MAPK7* of all of the cell lines tested. These findings suggest that increased levels of ERK5 enhance the growth of HCC cells. Moreover, our results indicate that ERK5 is phosphorylated during the G2/M phases of the cell cycle and that it regulates entry into mitosis, which may explain how it promotes the growth of HCC cells.

Conflicting results have been reported by different investigators regarding the role of ERK5 in cell cycle progression. Some investigators have reported that ERK5 regulates the G1/S transition: expression of a dominant-negative form of ERK5 prevents cells from entering the S-phase of the cell cycle (Kato et al., 1998), and ERK5 can drive cyclin D1 expression (Mulloy et al., 2003). In contrast, Cude et al., (2007) and Gírio et al., (2007) recently reported that ERK5 is activated at the G2/M phases and is required for mitotic entry, findings that agree with our results.

Few molecules have been identified as direct downstream targets of ERK5. The transcriptional factors of the monocyte enhancer factor 2 family are among the best characterized substrates of ERK5. Phosphorylation of monocyte enhancer factor 2C by ERK5 enhances its transcriptional activity and subsequently leads to an increase in c-Jun gene expression (Kato et al., 1997; Wang and Tournier, 2006). A more complete identification of components downstream of ERK5 will be necessary to fully understand the role of ERK5 in carcinogenesis.

In summary, using high-density SNP arrays, we identified *MAPK7* as a probable target for the amplification events at 17p11 in HCCs. Our results suggest that the ERK5 protein product of the *MAPK7* gene plays a role in proliferation of HCC cells by regulating mitotic entry and may therefore be an optimal target for the development of novel therapies for this widespread type of cancer.

REFERENCES

Aden DP, Fogel A, Plotkin S, Damjanov I, Knowles BB. 1979. Controlled synthesis of HBsAg in a differentiated human liver carcinoma-derived cell line. Nature 282:615–616.

Alexander JJ, Bey EM, Geddes EW, Lecatsas G. 1976. Establishment of a continuously growing cell line from primary carcinoma of the liver. S Afr Med J 50:2124–2128.

Bignell GR, Huang J, Greshock J, Watt S, Butler A, West S, Grigorova M, Jones KW, Wei W, Stratton MR, Futreal PA, Weber B, Shapero MH, Wooster R. 2004. High-resolution analysis of DNA copy number using oligonucleotide microarrays. Genome Res 14:287–295.

Buschbeck M, Hofbauer S, Di Croce L, Keri G, Ullrich A. 2005. Abl-kinase-sensitive levels of ERK5 and its intrinsic basal activity contribute to leukaemia cell survival. EMBO Rep 6:63–69.

Carvajal-Vergara X, Tabera S, Montero JC, Esparís-Ogando A, López-Pérez R, Mateo G, Gutiérrez N, Parmo-Cabañas M, Teixidó J, San Miguel JF, Pandiella A. 2005. Multifunctional role of Erk5 in multiple myeloma. Blood 105:4492–4499.

Chiariello M, Marinissen MJ, Gutkind JS. 2000. Multiple mitogen-activated protein kinase signaling pathways connect the cot oncoprotein to the c-jun promoter and to cellular transformation. Mol Cell Biol 20:1747–1758.

Collins C, Rommens JM, Kowbel D, Godfrey T, Tanner M, Hwang SI, Polikoff D, Nonet G, Cochran J, Myambo K, Jay KE, Froula J, Cloutier T, Kuo WL, Yaswen P, Dairkee S, Giovanola J, Hutchinson GB, Isola J, Kallioniemi OP, Palazzolo M, Martin C, Ericsson C, Pinkel D, Albertson D, Li WB, Gray JW. 1998. Positional cloning of ZNF217 and NABC1: Genes amplified at 20q13.2 and overexpressed in breast carcinoma. Proc Natl Acad Sci USA 95:8703–8708.

Cude K, Wang Y, Choi HJ, Hsuan SL, Zhang H, Wang CY, Xia Z. 2007. Regulation of the G2-M cell cycle progression by the ERK5-NFkappaB signaling pathway. J Cell Biol 177:253–264.

Di Fiore PP, Pierce JH, Kraus MH, Segatto O, King CR, Aaronson SA. 1987. erbB-2 is a potent oncogene when overexpressed in NIH/3T3 cells. Science 237:178–182.

Di X, Matsuzaki H, Webster TA, Hubbell E, Liu G, Dong S, Bartell D, Huang J, Chiles R, Yang G, Shen MM, Kulp D, Kennedy GC, Mei R, Jones KW, Cawley S. 2005. Dynamic model based algorithms for screening and genotyping over 100 K SNPs on oligonucleotide microarrays. Bioinformatics 21:1958–1963.

Dor I, Namba M, Sato J. 1975. Establishment and some biological characteristics of human hepatoma cell lines. Gann 66:385–392.

El-Serag HB. 2002. Hepatocellular carcinoma: An epidemiologic view. J Clin Gastroenterol 35:S72–S78.

English JM, Pearson G, Hockenberry T, Shivakumar L, White MA, Cobb MH. 1999. Contribution of the ERK5/MEK5 pathway to Ras/Raf signaling and growth control. J Biol Chem 274:31588–1592.

Esparis-Ogando A, Diaz-Rodriguez E, Montero JC, Yuste L, Crespo P, Pandiella A. 2002. Erk5 participates in neuregulin signal transduction and is constitutively active in breast cancer cells overexpressing ErbB2. Mol Cell Biol 22:270–285.

Forus A, Weghuis DO, Smeets D, Fodstad O, Myklebost O, Geurts van Kessel A. 1995. Comparative genomic hybridization analysis of human sarcomas. II. Identification of novel amplicons at 6p and 17p in osteosarcomas. Genes Chromosomes Cancer 14:15–21.

Fujise K, Nagamori S, Hasumura S, Homma S, Sujino H, Matsuura T, Shimizu K, Niiya M, Kameda H, Fujita K. 1990. Integration of hepatitis B virus DNA into cells of six established human hepatocellular carcinoma cell lines. Hepatogastroenterology 37:457–460.

Garaude J, Cherni S, Kaminski S, Delepine E, Chable-Bessia C, Benkirane M, Borges J, Pandiella A, Iñiguez MA, Fresno M, Hipskind RA, Villalba M. 2006. ERK5 activates NF-kappaB in leukemic T cells and is essential for their growth in vivo. J Immunol 177:7607–7617.

Garraway LA, Widlund HR, Rubin MA, Getz G, Berger AJ, Ramaswamy S, Beroukhim R, Milner DA, Granter SR, Du J, Lee C, Wagner SN, Li C, Golub TR, Rimm DL, Meyerson ML, Fisher DE, Sellers WR. 2005. Integrative genomic analyses identify MITF as a lineage survival oncogene amplified in malignant melanoma. Nature 436:117–122.

Gírio A, Montero JC, Pandiella A, Chatterjee S. 2007. Erk5 is activated and acts as a survival factor in mitosis. Cell Signal 19:1964–1972.

Hayashi M, Lee JD. 2004. Role of the BMK1/ERK5 signaling pathway: Lessons from knockout mice. J Mol Med 82:800–808.

Hirohashi S, Shimosato Y, Kameya T, Koide T, Mukojima T, Taguchi Y, Kageyama K. 1979. Production of -fetoprotein and normal serum proteins by xenotransplanted human hepatomas in relation to their growth and morphology. Cancer Res 39: 1819–1828.

Huh N, Utakoji T. 1981. Production of HBs-antigen by two new human hepatoma cell lines and its enhancement by dexamethasone. Gann 72:178–179.

Kallioniemi A, Kallioniemi OP, Sudar D, Rutovitz D, Gray JW, Waldman F, Pinkel D. 1992. Comparative genomic hybridization for molecular cytogenetic analysis of solid tumors. Science 258:818–821.

Kato Y, Kravchenko VV, Tapping RI, Han J, Ulevitch RJ, Lee JD. 1997. BMK1/ERK5 regulates serum-induced early gene expression through transcription factor MEF2C. EMBO J 16:7054–7066.

Kato Y, Tapping RI, Huang S, Watson MH, Ulevitch RJ, Lee JD. 1998. Bmk1/Erk5 is required for cell proliferation induced by epidermal growth factor. Nature 395:713–716.

Kennedy GC, Matsuzaki H, Dong S, Liu WM, Huang J, Liu G, Su X, Cao M, Chen W, Zhang J, Liu W, Yang G, Di X, Ryder T, He Z, Surti U, Phillips MS, Boyce-Jacino MT, Fodor SP, Jones KW. 2003. Large-scale genotyping of complex DNA. Nat Biotechnol 21:1233–1237.

Knowles BB, Howe CC, Aden DP. 1980. Human hepatocellular carcinoma cell lines secrete the major plasma proteins and hepatitis B surface antigen. Science 209:97–499.

Linnerth NM, Baldwin M, Campbell C, Brown M, McGowan H, Moorehead RA. 2005. IGF-II induces CREB phosphorylation and cell survival in human lung cancer cells. Oncogene 24:7310–7319.

Little CD, Nau MM, Carney DN, Gazdar AF, Minna JD. 1983. Amplification and expression of the c-myc oncogene in human lung cancer cell lines. Nature 306:194–196.

Matsuzaki H, Dong S, Loi H, Di X, Liu G, Hubbell E, Law J, Berntsen T, Chadha M, Hui H, Yang G, Kennedy GC, Webster TA, Cawley S, Walsh PS, Jones KW, Fodor SP, Mei R. 2004a. Genotyping over 100,000 SNPs on a pair of oligonucleotide arrays. Nat Methods 1:109–111.

Matsuzaki H, Loi H, Dong S, Tsai YY, Fang J, Law J, Di X, Liu WM, Yang G, Liu G, Huang J, Kennedy GC, Ryder TB, Marcus GA, Walsh PS, Shriver MD, Puck JM, Jones KW, Mei R. 2004b. Parallel genotyping of over 10,000 SNPs using a one-primer assay on a high-density oligonucleotide array. Genome Res 14:414–425.

McCracken SR, Ramsay A, Heer R, Mathers ME, Jenkins BL, Edwards J, Robson CN, Marquez R, Cohen P, Leung HY. 2008. Aberrant expression of extracellular signal-regulated kinase 5 in human prostate cancer. Oncogene 27:2978–2988.

Mehta PB, Jenkins BL, McCarthy L, Thilak L, Robson CN, Neal DE, Leung HY. 2003. MEK5 overexpression is associated with metastatic prostate cancer, and stimulates proliferation, MMP-9 expression and invasion. Oncogene 22:1381–1389.

Mei R, Galipeau PC, Prass C, Berno A, Ghandour G, Patil N, Wolff RK, Chee MS, Reid BJ, Lockhart DJ. 2000. Genome-wide detection of allelic imbalance using human SNPs and high-density DNA arrays. Genome Res 10:1126–1137.

Minamiya Y, Matsuzaki I, Sageshima M, Saito H, Taguchi K, Nakagawa T, Ogawa J. 2004. Expression of tissue factor mRNA and invasion of blood vessels by tumor cells in non-small cell lung cancer. Surg Today 34:1–5.

Mulloy R, Salinas S, Philips A, Hipskind RA. 2003. Activation of cyclin D1 expression by the ERK5 cascade. Oncogene 22:5387–5398.

Nakabayashi H, Taketa K, Miyano K, Yamane T, Sato J. 1982. Growth of human hepatoma cells lines with differentiated functions in chemically defined medium. Cancer Res 42:3858–3863.

Nannya Y, Sanada M, Nakazaki K, Hosoya N, Wang L, Hangaishi A, Kurokawa M, Chiba S, Bailey DK, Kennedy GC, Ogawa S. 2005. A robust algorithm for copy number detection using high-density oligonucleotide single nucleotide polymorphism genotyping arrays. Cancer Res 65:6071–6079.

Nishimoto S, Nishida E. 2006. MAPK signalling: ERK5 versus ERK1/2. EMBO Rep 7:782–786.

Okamoto H, Yasui K, Zhao C, Arii S, Inazawa J. 2003. PTK2 and EIF3S3 genes may be amplification targets at 8q23-q24 and are associated with large hepatocellular carcinomas. Hepatology 38:1242–1249.

Park JG, Lee JH, Kang MS, Park KJ, Jeon YM, Lee HJ, Kwon HS, Park HS, Yeo KS, Lee KU, Kim ST, Chung JK, Hwang YJ, Lee HS, Kim CY, Lee YI, Chen TR, Hay RJ, Song SY, Kim WH, Kim CW, Kim YI. 1995. Characterization of cell lines established from human hepatocellular carcinoma. Int J Cancer 62:276–282.

Rosenthal JA, Chen H, Slepnev VI, Pellegrini L, Salcini AE, Di Fiore PP, De Camilli P. 1999. The epsins define a family of proteins that interact with components of the clathrin coat and contain a new protein module. J Biol Chem 274:33959–33965.

Sun W, Wei X, Kesavan K, Garrington TP, Fan R, Mei J, Anderson SM, Gelfand EW, Johnson GL. 2003. MEK kinase 2 and the adaptor protein Lad regulate extracellular signal-regulated kinase 5 activation by epidermal growth factor via Src. Mol Cell Biol 23:2298–2308.

Tarkkanen M, Karhu R, Kallioniemi A, Elomaa I, Kivioja AH, Nevalainen J, Böhling T, Karaharju E, Hyytinen E, Knuutila S, Kallioniemi OP. 1995. Gains and losses of DNA sequences in osteosarcomas by comparative genomic hybridization. Cancer Res 55:1334–1338.

van Dartel M, Cornelissen PW, Redeker S, Tarkkanen M, Knuutila S, Hogendoorn PC, Westerveld A, Gomes I, Bras J, Hulsebos TJ. 2002. Amplification of 17p11.2 approximately p12, including PMP22, TOP3A, and MAPK7, in high-grade osteosarcoma. Cancer Genet Cytogenet 139:91–96.

Wang X, Tournier C. 2006. Regulation of cellular functions by the ERK5 signalling pathway. Cell Signal 18:753–760.

Weldon CB, Scandurro AB, Rolfe KW, Clayton JL, Elliott S, Butler NN, Melnik LI, Alam J, McLachlan JA, Jaffe BM, Beckman BS, Burow ME. 2002. Identification of mitogen-activated protein kinase kinase as a chemoresistant pathway in MCF-7 cells by using gene expression microarray. Surgery 132:293–301.

Wong KK, Tsang YT, Shen J, Cheng RS, Chang YM, Man TK, Lau CC. 2004. Allelic imbalance analysis by high-density single-nucleotide polymorphic allele (SNP) array with whole genome amplified DNA. Nucleic Acids Res 32:e69.

Yasui K, Arii S, Zhao C, Imoto I, Ueda M, Nagai H, Emi M, Inazawa J. 2002. TFDP1, CUL4A, and CDC16 identified as targets for amplification at 13q34 in hepatocellular carcinomas. Hepatology 35:1476–1484.

Yasui K, Imoto I, Fukuda Y, Pimkhaokham A, Yang ZQ, Naruto T, Shimada Y, Nakamura Y, Inazawa J. 2001. Identification of target genes within an amplicon at 14q12-q13 in esophageal squamous cell carcinoma. Genes Chromosomes Cancer 32:112–118.

Yokoi S, Yasui K, Iizasa T, Imoto I, Fujisawa T, Inazawa J. 2003. TERC identified as a probable target within the 3q26 amplicon that is detected frequently in non-small cell lung cancers. Clin Cancer Res 9:4705–4713.

Yokoi S, Yasui K, Saito-Ohara F, Koshikawa K, Iizasa T, Fujisawa T, Terasaki T, Horii A, Takahashi T, Hirohashi S, Inazawa J. 2002. A novel target gene, SKP2, within the 5p13 amplicon that is frequently detected in small cell lung cancers. Am J Pathol 161:207–216.

Yuste L, Montero JC, Esparis-Ogando A, Pandiella A. 2005. Activation of ErbB2 by overexpression or by transmembrane neuregulin results in differential signaling and sensitivity to herceptin. Cancer Res 65:6801–6810.

Zhao X, Li C, Paez JG, Chin K, Jänne PA, Chen TH, Girard L, Minna J, Christiani D, Leo C, Gray JW, Sellers WR, Meyerson M. 2004. An integrated view of copy number and allelic alterations in the cancer genome using single nucleotide polymorphism arrays. Cancer Res 64:3060–3071.

Zhao X, Weir BA, LaFramboise T, Lin M, Beroukhim R, Garraway L, Beheshti J, Lee JC, Naoki K, Richards WG, Sugarbaker D, Chen F, Rubin MA, Jänne PA, Girard L, Minna J, Christiani D, Li C, Sellers WR, Meyerson M. 2005. Homozygous deletions and chromosome amplifications in human lung carcinomas revealed by single nucleotide polymorphism array analysis. Cancer Res 65:5561–5570.

DOI 10.1002/prca.200900112 *Proteomics Clin. Appl.* 2009, *3*, 1256–1264

RESEARCH ARTICLE

Heterogeneous expressions of hepcidin isoforms in hepatoma-derived cells detected using simultaneous LC-MS/MS

Takaaki Hosoki[1], Katsuya Ikuta[1], Yasushi Shimonaka[2], Yusuke Sasaki[2], Hideyuki Yasuno[2], Kazuya Sato[1], Takaaki Ohtake[1], Katsunori Sasaki[3], Yoshihiro Torimoto[4], Keiji Saito[2] and Yutaka Kohgo[1]

[1] Division of Gastroenterology and Hematology/Oncology, Department of Medicine, Asahikawa Medical College, Asahikawa, Japan
[2] Kamakura Research Labs, Chugai Pharmaceutical Co., Ltd., Kamakura, Japan
[3] Department of Gastrointestinal Immunology and Regenerative Medicine, Asahikawa Medical College, Asahikawa, Japan
[4] Oncology Center, Asahikawa Medical College Hospital, Asahikawa, Japan

Received: June 3, 2009
Revised: July 13, 2009
Accepted: July 17, 2009

Hepcidin, a key regulator of iron homeostasis, is known to have three isoforms: hepcidin-20, -22, and -25. Hepcidin-25 is thought to be the major isoform and the only one known to be involved in iron metabolism; the physiological roles of other isoforms are poorly understood. Because of its involvement in the pathophysiology of hereditary hemochromatosis and the anemia of chronic disease, the regulatory mechanisms of hepcidin expression have been extensively investigated, but most studies have been performed only at the transcriptional level. Difficulty in detecting hepcidin has impeded *in vitro* research. In the present study, we developed a novel method for simultaneous quantification of hepcidin-20, -22, and -25 in the media from hepatoma-derived cell lines. Using this method, we determined the expression patterns of hepcidin isoforms and the patterns of responses to various stimuli in human hepatoma-derived cultured cells. We found substantial differences among cell lines. In conclusion, a novel method for simultaneous quantification of hepcidin isoforms is presented. Heterogeneous expressions of hepcidin isoforms in human hepatoma-derived cells were revealed by this method. We believe our method will facilitate quantitative investigation of the role hepcidin plays in iron homeostasis.

Keywords:
Hepatocyte / Hepcidin antimicrobial peptide / Iron metabolism / LC-MS/MS

Correspondence: Dr. Katsuya Ikuta, Division of Gastroenterology and Hematology/Oncology, Department of Medicine, Asahikawa Medical College, 2-1-1-1 Midorigaoka-Higashi, Asahikawa, Hokkaido 078-8510, Japan
E-mail: ikuta@asahikawa-med.ac.jp
Fax: +81-166-68-2469

Abbreviations: **Ct**, threshold cycle; **DFO**, desferrioxamine; **EMEM**, Eagle's minimum essential medium; **FAC**, ferric ammonium citrate; **HAMP**, hepcidin antimicrobial peptide; **holo-Tf**, holo-transferrin; **IL-1β**, interleukin-1β; **IL-6**, interleukin-6; **LPS**, lipopolysaccharide; **QC**, quality control; **qRT-PCR**, quantitative RT-PCR; **SRM**, selected reaction monitoring

1 Introduction

Hepcidin is a small peptide mainly produced by the liver, and it is thought to be the key regulator in iron homeostasis [1, 2]. Hepcidin binds to ferroportin, the mammalian iron exporter expressed on the basolateral side of enterocytes and on the cell surface of macrophages, thereby causing the internalization and degradation of ferroportin [3]. Hepcidin thus inhibits iron uptake from the gastrointestinal tract and iron release from reticuloendothelial cells, so that iron balance of the body is negatively regulated by hepcidin [1, 2]. Increased

© 2009 WILEY-VCH Verlag GmbH & Co. KGaA, Weinheim

hepcidin expression therefore leads to iron deficiency while decreased hepcidin expression causes iron overload.

Hepcidin is involved in several diseases, such as hereditary hemochromatosis and the anemia of chronic disease. In hereditary hemochromatosis, various mutations occur in genes such as *HFE*, *hemojuvelin*, and *transferrin receptor 2*, leading to decreased hepcidin expression despite generalized iron overload [4–6]. In contrast, in anemia of chronic disease, inflammatory cytokines such as interleukin-6 (IL-6) [7, 8] and interleukin-1β (IL-1β) [9, 10] upregulate hepcidin expression and thus cause iron-deficiency anemia.

Recently, the regulation of hepcidin expression has been intensively studied to reveal pathophysiological mechanisms involved in diseases in which iron metabolism is altered. For instance, the cytokine IL-6 increases hepcidin synthesis utilizing signal transducers and activators of transcription-3 during inflammation such as caused by systemic infections [11]. The bone morphogenic proteins (BMPs) are members of the transforming growth factor β superfamily, and BMPs have been proposed to be involved in hemojuvelin-mediated regulation of hepcidin synthesis [12]. However, almost all research on the regulation of hepcidin expression has been restricted to studying changes in transcription of the *hepcidin antimicrobial peptide* (*HAMP*) gene utilizing RT-PCR under various conditions.

Hepcidin is produced mainly by hepatocytes expressing the *HAMP* gene located on chromosome 19. The transcript of this gene is believed to produce a prepropeptide of 84 amino acids, and then the peptide is digested by furin, the intercellular convertase, and finally the mature form of hepcidin appears in the peripheral blood [13]. However, there is little information about the ratios of serum prohepcidin to mature hepcidin, and the secreted fraction of hepcidin to hepcidin retained intracellularly. In addition, kidney cells have been shown to produce hepcidin independently of the liver [14]. Therefore, there is no proof that *HAMP* transcript levels of the liver reflect total body secretion of hepcidin-25. Consequently, it is desirable that hepcidin be determined from peptide levels in the serum, in addition to transcriptional levels of the liver and other organs.

Three isoforms of mature hepcidin are known. A 25-amino acid peptide (hepcidin-25) is thought to be the major isoform [15], but other forms of hepcidin such as hepcidin-20 and -22 have been detected in human urine [16]. Only hepcidin-25 has been shown to cause the internalization and degradation of ferroportin. However, the possibility arises that hepcidin-20 and -22 have different physiological roles in homeostasis and their expressions are regulated independently from hepcidin-25. It is therefore desirable that hepcidin-20, -22, and -25 be separately quantified.

The first method for measuring prohepcidin, using ELISA, was reported by Kulaksiz *et al.* [17]. That method has been applied for the analysis of hepcidin expression levels, but there is little information about how and whether hepatocytes secrete prohepcidin into the blood [17]. Several groups have developed antibodies to detect and measure hepcidin, but difficulties for differentiation of hepcidin-20, -22, and -25 [18] persist. MS-based modalities have been used in recent years for measuring hepcidin. For instance, SELDI-TOF-MS has been used for semi-quantification [19, 20], and LC-MS/MS has been employed for quantification of hepcidin [21, 22]. These methods are applicable to assaying clinical samples such as blood and urine. Most recently, Ganz *et al.* reported development of an ELISA system for quantification of human serum hepcidin that is expected to be a powerful tool for clinical samples [23].

Experiments *in vitro* would also be valuable for investigating the complex molecular mechanisms regulating hepcidin expression. Detection and quantification of hepcidin in cell culture media has been difficult, probably due to its low concentration.

We therefore aimed to develop a sensitive new method for measuring hepcidin that can simultaneously measure hepcidin-20, -22, and -25 secreted in culture media by hepatoma-derived cells. We now report such a method, improving the MS-based modality that we previously reported [22]. We also determined the characteristics of hepcidin expression of various hepatoma cell lines using the new method, which can be applied to analyzing differences among hepatoma cells of varying lineage.

2 Materials and methods

2.1 Hepcidin standards

Human hepcidin-25 was obtained from the Peptide Institute (Osaka, Japan). Hepcidin-20, -22, and [$^{13}C_{18}$, $^{15}N_3$]-hepcidin-25 were synthesized at the Peptide Institute.

2.2 Chemicals

BMP2 and holo-transferrin (holo-Tf) were purchased from R & D Systems; IL-6 was obtained from Wako Pure Chemical Industries, Osaka, Japan. FBS was purchased from Japan Bioserum; Eagle's minimum essential medium (EMEM), DMEM, RPMI-1640 medium, L-glutamine, and sodium bicarbonate were purchased from Sigma-Aldrich. Penicillin–streptomycin solution were bought from Invitrogen. IL-1β was purchased from Wako Pure Chemical Industries; desferrioxamine (DFO), ferric ammonium citrate (FAC), lipopolysaccharide (LPS), and cobalt chloride were obtained from Sigma-Aldrich. Decanoyl-RVKR-CMK (furin inhibitor I) was purchased from Calbiochem (Darmstadt, Germany). All other chemicals and solvents were of analytical reagent grade.

2.3 Cell cultures

Human hepatoma-derived cell lines used in this study were HepG2, HuH-1, HuH-2, HuH-4, HuH-6, HuH-7, WRL68, HB611, Hep3B, HLE, HLF, SK-HEP-1, and human primary

© 2009 WILEY-VCH Verlag GmbH & Co. KGaA, Weinheim

hepatocytes derived from normal liver (Applied Cell Biology Research Institute).

HuH-4, HB611, and HuH-6 cells were incubated with RPMI1640; HuH-7 cells were incubated with DMEM. Other cells were incubated with EMEM. Those medium were supplemented with 10% FBS, 100 U/mL penicillin, and 100 μg/mL streptomycin. All cells were cultured at 37°C in a humidied incubator with 5% CO_2. In some experiments, FBS-free UltraCulture medium (Lonza, MD, USA) supplemented with 2 mM L-glutamine was used. HepG2 cells could survive in this serum-free medium for more than 3 days.

Cells at the density of 1×10^6 cells/mL were grown in 6-well plates for 24 h to almost 80% conuency in 2 mL of culture medium. Medium in each well was replaced by 2 mL of culture medium containing various stimulants and then incubated for 48 h. All cell lines were maintained with 20 ng/mL IL-6 or 30 μM holo-Tf or no additives for control cells.

After 48 h, culture media were collected and analyzed for hepcidin-20, -22, and -25 concentrations as follows: 50 μL of 4% trichloroacetic acid solution containing 200 ng/mL [$^{13}C_{18}$, $^{15}N_3$]-hepcidin-25 as internal standard was added to an equal amount of each culture medium, mixed vigorously, and centrifuged. A 20-μL aliquot of the resulting supernatant was analyzed quantitatively by LC-MS/MS. Cells were lysed with 0.1% Triton X-100 for protein assay, or by Sepazol™ (Nacarai Tesque, Japan) for RT-PCR studies.

HepG2 cells were also treated with various reagents instead of IL-6 or holo-Tf, such as 200 pg/mL IL-1β, 100 μM DFO, 100 μM FAC, 1 μg/mL LPS, 50 μM $CoCl_2$, or 50 μM furin inhibitor I. After 48 h, culture media were collected for quantification of hepcidin isoforms, and cells were lysed for measuring protein concentrations.

Each treatment was performed in triplicate, and data presented as mean and SD.

2.4 LC/ESI-MS/MS analysis

LC/ESI-MS/MS was performed using an API4000QTRAP (Applied Biosystems, Foster City, CA, USA) equipped with a UPLC ACQUITY™ systems (Waters). The turboionspray was operated in the positive ion mode at 5500 V for the ion spray voltage. Analytical chromatography of human hepcidin-20, -22, and -25 was accomplished on a PLRP-S column (5 μm, 300 Å, 150 mm × 2.0 mm id; Polymer Laboratories, Shropshire, UK). Instrument control and data processing were with Analyst™ software version 1.4 (Applied Biosystems).

2.5 Quantitative analysis of human hepcidin-20, -22, and -25

Selected reaction monitoring (SRM) transitions were as follows: human hepcidin-20, m/z 548.85 → 119.80; human hepcidin-22, m/z 610.14 → 119.80; human hepcidin-25, m/z 558.80 → 120.07; [$^{13}C_{18}$, $^{15}N_3$]-human hepcidin-25, m/z 563.11 → 109.60. The declustering potential for human hepcidin-20, -22, -25, and [$^{13}C_{18}$, $^{15}N_3$]-human hepcidin-25 were 50, 50, 81, and 81 V, respectively. The turboionspray source was maintained at a temperature of 600°C. Collision energies for human hepcidin-20, -22, -25, and [$^{13}C_{18}$, $^{15}N_3$]-human hepcidin-25 were 52, 59, 73 and 75 V, respectively. The collisional activation dissociation gas was set at 4. Mobile phase A was 0.1% aqueous formic acid, and mobile phase B was 0.1% formic acid in ACN. Gradient conditions were as follows: B 20% (0 min, 0.3 mL/min) → 20% (2.01 min, 0.3 mL/min) → 25% (5.00 min, 0.3 mL/min) → 25% (10.00 min, 0.3 mL/min) → 90% (10.01 min, 0.3 mL/min) → 90% (12.00 min, 0.3 mL/min) → 20% (12.01 min, 0.3 mL/min) → 20% (14.00 min, 0.3 mL/min).

Analysis of hepcidin-25 in the BMP2-stimulated HepG2 culture medium was performed on the 6520 quadrupole-TOF/MS (Agilent Technologies).

2.6 RNA isolation and quantitative RT-PCR

Total RNA was isolated and quantitative RT-PCR (qRT-PCR) was performed in a reaction mix containing TaqMan Universal PCR Master Mix No AmpErase UNG (Applied Biosystems), specific human *HAMP* primers, and probe (pre-validated Taqman gene expression assay, Applied Biosystems), and 100 ng of cDNA. All reactions were multiplexed with the housekeeping gene 18S, provided as a pre-optimized control probe (Applied Biosystems) enabling data to be expressed as delta threshold cycle (ΔCt) values (where ΔCt = Ct of 18 s subtracted from Ct of gene of interest). Reactions were as follows: 50°C for 2 min, 95°C for 10 min; then 60 cycles of 95°C for 15 s and 60°C for 1 min. All measurements were performed in triplicate, and relative *HAMP* mRNA expression was expressed as fold expression over the average of *HAMP* mRNA expression corresponding to the HepG2 cells.

2.7 Cellular protein assay

Cell were lysed with 0.1% Triton-X and total protein concentrations were determined using the Bradford reagent (BioRad, Hercules, CA, USA), following the manufacturer's instructions.

3 Results

3.1 Establishment of quantitative measurement of hepcidin isoforms

To improve further the method for quantifying small peptides by LC-MS/MS, we developed a quantitative and simultaneous method for hepcidin-20, -22, and -25 in

© 2009 WILEY-VCH Verlag GmbH & Co. KGaA, Weinheim

biological fluids. Upon optimization of SRM conditions, the most intense precursor ions were selected in each mass spectrum to detect hepcidin isoforms. Product ions were selected to maximize sensitivity and selectivity. Using EMEM supplemented with 10% FBS as matrix, various concentrations of synthetic hepcidin isoforms were spiked, and analyzed by LC-MS/MS. Isoform peaks were not interfered with by a blank matrix, indicating the method has good selectivity.

Our method was validated by specificity, linearity, lower limit of quantification, intra-assay precision, and accuracy. Calibration curves were constructed over the range 2–1000 ng/mL in the above matrix. Five replicates of 2, 5, 50, 500, and 1000 ng/mL of each isoform quality control (QC) samples were prepared and analyzed by LC-MS/MS.

There was no interference peak at retention time of each isoform, confirming good specificity (Fig. 1A). Linearity of the calibration curves by weighted ($1/x^2$) linear regression was excellent (correlation coefficient: $r = 0.9974$ for hepcidin-20, $r = 0.9937$ for hepcidin-22, $r = 0.9950$ for hepcidin-25; Fig. 1B). Accuracies of the back-corrected concentrations were within 87.4–109% for hepcidin-20, 80.1–110% for hepcidin-22, and 80.5–109% for hepcidin-25. The lower limits of quantification for each hepcidin isoform was 2 ng/mL. Coefficients of variance in intra-assay QC samples were 1.2–8.6% for hepcidin-20, 3.1–5.7% for hepcidin-22, and 1.5–7.0% for hepcidin-25. Accuracies for QC samples were 99.7–122.1% for hepcidin-20, 102.6–132.5% for hepcidin-22, and 99.1–141.2% for hepcidin-25. These results indicate that the method is adequate for quantifying hepcidin isoforms in culture media.

3.2 Detection of hepcidin isoforms in HepG2 media

In the SRM chromatogram of HepG2 medium analyzed by LC-MS/MS, peaks corresponding to the retention time of synthetic hepcidin-22 and -25, but not hepcidin-20, were detected. Peaks corresponding to hepcidin-22 and -25 were also detected and up-regulated in 100 ng/mL BMP2 stimulated HepG2 medium (Fig. 2A). No peaks corresponding to hepcidin-20 were founded in the chromatogram of HepG2 media at any tested conditions.

We tried to identify the component of the corresponding peak for hepcidin-25 in HepG2 medium. For that purpose, BMP2 medium was prepared because it contained a relatively high concentration of putative hepcidin-25, (65.9 ng/mL). Synthetic hepcidin-25 and BMP2 medium were analyzed by quadrupole-TOF/MS. The major precursor ions of synthetic hepcidin-25 ranged from $m/z = 558.4$–559.0. At the same retention time, precursor ions from BMP2 medium showed a similar distribution (Fig. 2B). Mass spectra of product ions were also similar. Several major common product ions were observed (Fig. 2C). Overall, synthetic hepcidin-25 and HepG2-derived peak components are similar in retention time and mass spectra of the

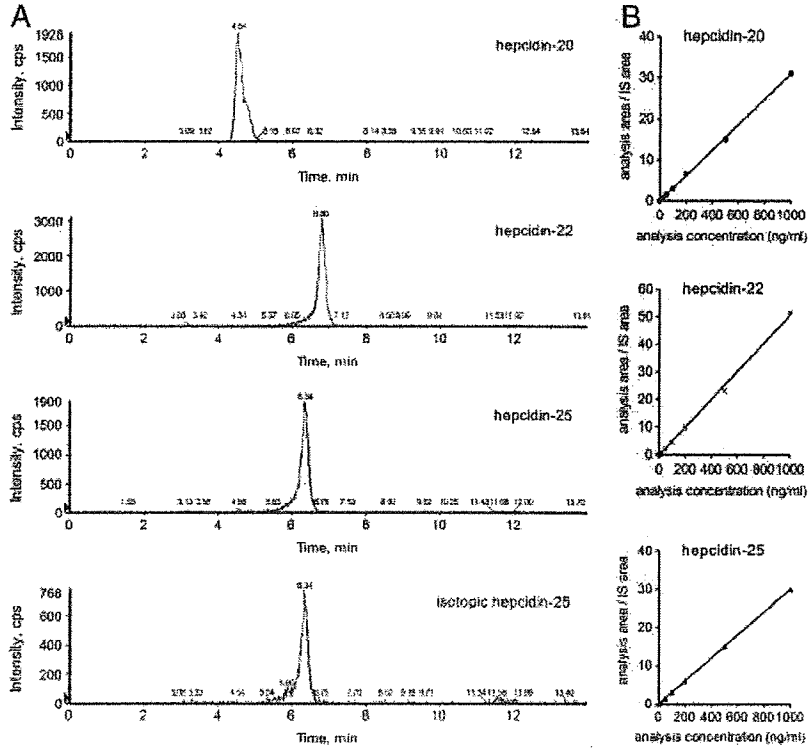

Figure 1. (A) Representative LC-MS/MS chromatograms of hepcidin-20, -22, -25, and blank isotopic hepcidin-25 sample. (B) The calibration curves of hepcidin-20, -22, and -25 in the culture medium are linear in the range of 2–1000 ng/mL. The correlation coefficients of calibration curves are as follows: hepcidin-20, $r = 0.9974$; hepcidin-22, $r = 0.9937$; hepcidin-25, $r = 0.9950$.

© 2009 WILEY-VCH Verlag GmbH & Co. KGaA, Weinheim

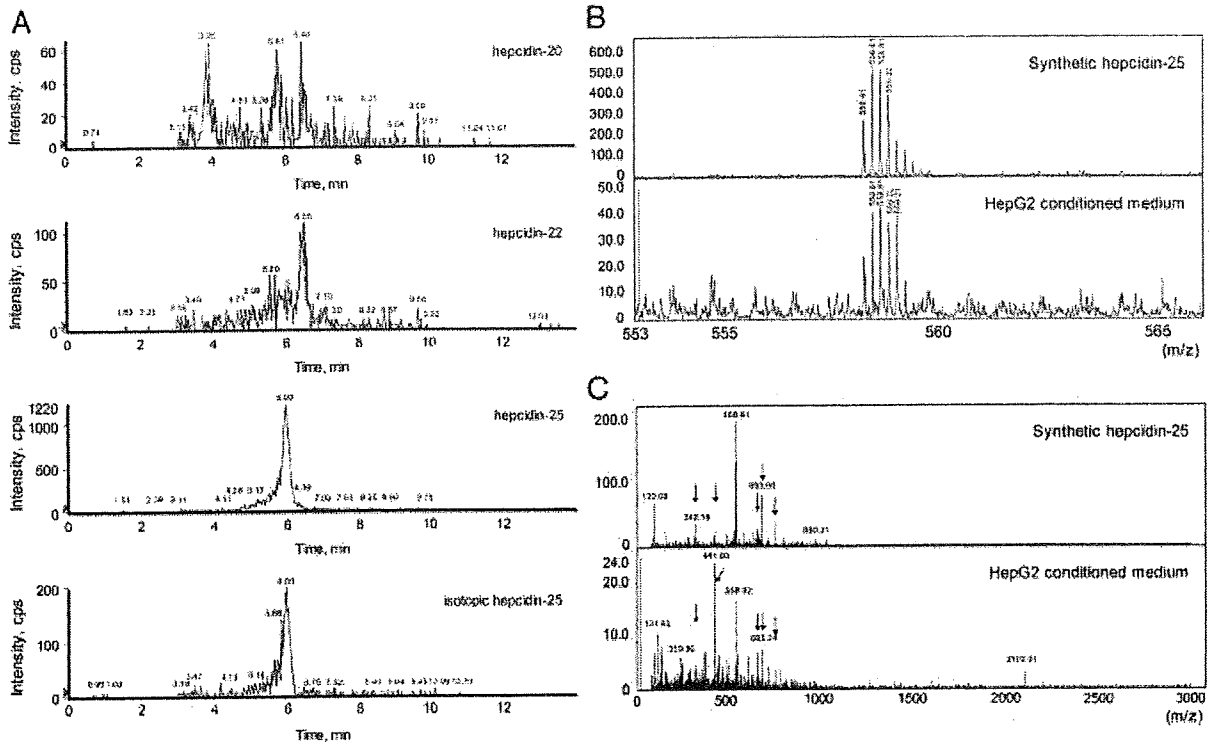

Figure 2. (A) Detection of hepcidin isoforms in BMP2-stimulated HepG2 medium. (B) MS spectra of synthetic hepcidin-25 and derived peak from BMP2-stimulated HepG2 medium showing similar patterns. (C) MS/MS spectra of synthetic hepcidin-25 and derived peak from BMP2-stimulated HepG2 medium showing similar patterns. Arrows show common fragments.

precursor ions and product ions, verifying that the peak detected in the culture medium represents hepcidin-25.

3.3 HAMP gene expressions in hepatoma-derived cell lines

We aimed at first to determine qualitatively whether cell lines derived from hepatocellular carcinomas express the *HAMP* gene as assayed by RT-PCR. Expression levels of *HAMP* mRNA differed among cell lines (Fig. 3A). HepG2, HuH-1, and HuH-7 cells showed relatively high *HAMP* mRNA expressions, but other cells exhibited only slight expressions. qRT-PCR was then performed (Fig. 3B). HepG2, HuH-1, and HuH-7 cells expressed high levels of *HAMP* mRNA, compatible with the results of qualitative RT-PCR. Only slight or moderate *HAMP* mRNA expression was found in other cells.

3.4 Quantification of hepcidin isoforms in the culture medium of various hepatoma-derived cell lines

HLE, HLF, SK-Hep1, and human primary hepatocytes did not show any detectable hepcidin isoforms in their culture media (data not shown). We could observe hepcidin isoforms in culture media from other cell lines. We also found that hepatoma-derived cell lines exhibited different patterns of hepcidin isoform expression and changes induced by various stimulations. Even among cell lines that secrete detectable hepcidin isoforms, four distinct patterns were discerned.

HepG2 cells expressed hepcidin-22 and -25, but not hepcidin-20. IL-6 significantly upregulated the expression of both isoforms, but holo-Tf suppressed hepcidin-25 expression (Fig. 4A).

WRL68 cells showed expression of hepcidin-20 and -22 even in control conditions, and holo-Tf stimulation increased both expressions significantly (Fig. 4B).

HuH-1 and HuH-7 cells expressed only hepcidin-25. IL-6 significantly increased the expression of hepcidin-25 in both cell lines. Addition of holo-Tf to the medium did not change the level of hepcidin-25 in HuH-1 cells, and even decreased hepcidin-25 in HuH-7 cells (Fig. 4C).

HB611, Hep3B, HuH-2, HuH-4, and HuH-6 showed expression of only hepcidin-20, but when holo-Tf was added, hepcidin-22 appeared (Fig. 4D).

We observed that some cell lines respond to holo-Tf by increasing the secretion of hepcidin-20 or -22. Although Lin *et al.* have reported *HAMP* mRNA expressions to be increased in mouse primary hepatocytes stimulated with

© 2009 WILEY-VCH Verlag GmbH & Co. KGaA, Weinheim

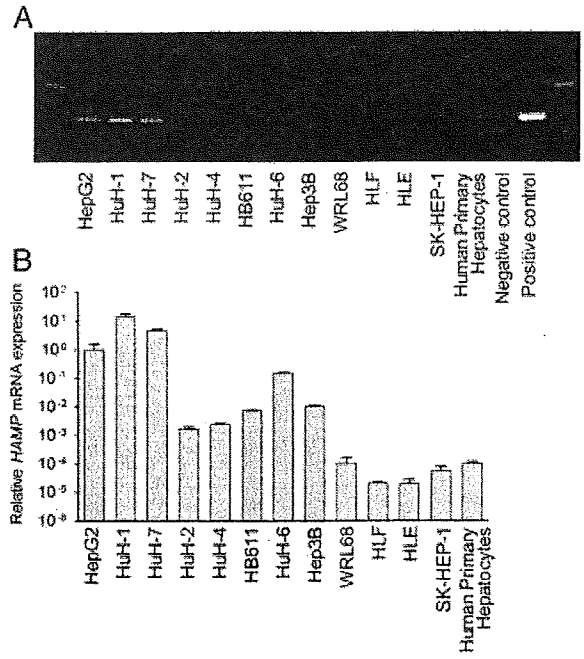

Figure 3. Expressions of *HAMP* mRNA in hepatoma-derived cell lines determined by qRT-PCR. (A) Qualitative RT-PCR showed that the expressions of *HAMP* mRNA were quite different among hepatoma-derived cell lines. (B) The expression levels of *HAMP* mRNA were standardized by 18*S* rRNA. Relative *HAMP* mRNA expression levels are shown as fold expression over the average of *HAMP* mRNA of HepG2 cells. HepG2, HuH-7, and HuH-1 cells highly express *HAMP* mRNA, while other cell lines exhibits only slight or moderate *HAMP* mRNA expressions.

human holo-Tf [24],] we believe ours is the first study showing upregulation of hepcidin at the peptide level by human holo-Tf in human cells. The physiological function of this effect is, however, not apparent since only hepcidin-25 is known to be involved in iron metabolism.

3.5 Determination of the changes of hepcidin expression in responses to various stimulations of HepG2 cells

The HepG2 cell line is one of the most frequently used hepatoma-derived lines for research and secretes mainly hepcidin-25, the only isoform reported to interact with ferroportin, into the culture medium.

Hepcidin expression has been reported to be regulated by inflammatory cytokines such as IL-6 and IL-1β; hence, HepG2 cells were stimulated with these cytokines. As shown in Fig. 5A, IL-6 significantly upregulates hepcidin-25, in agreement with earlier reports. A slight increase of hepcidin-22 was observed with IL-1β stimulation, but no obvious upregulation was seen in hepcidin-25. Iron overload has been reported to upregulate hepcidin expression *in vivo*, but addition of holo-Tf and FAC in the medium suppressed the expression of hepcidin-25. These results conflict with those of some *in vivo* investigations, but other transcriptional studies showed similar data to ours. Reasons for these discordances are still unknown.

Of interest, FAC increased hepcidin-22 expression by an unknown mechanism. DFO suppressed hepcidin-25 expression as expected change, but hepcidin-22 expression was increased. To investigate the effects of bacterial infections, LPS was added to media, and it significantly increased both hepcidin-22 and -25. Hypoxia is also reported to decrease hepcidin expressions [25], while in our studies $CoCl_2$ increased expression of both hepcidin-22 and -25. The furin inhibitor decreased hepcidin-25, but surprisingly hepcidin-22 was increased.

We then determined whether the inclusion of FBS influenced expressions of hepcidin types. Expressions of hepcidin-22 and -25 increased as higher concentrations of FBS were provided in the culture media, an effect that may have been due to the presence of cytokines in the FBS. HepG2 cells were then studied with various stimulants in FBS-free media. As shown in Fig. 5B, hepcidin expression levels were all lower than those determined in FBS-containing medium, and were almost at the limit of measurement by our method, but IL-6 upregulated hepcidin-25 expression. Holo-Tf and FAC depressed both hepcidin-22 and -25, as did the furin inhibitor. The finding that inclusion of FBS significantly influenced the expression of hepcidin deserves consideration from *in vitro* research using cultured cells.

4 Discussion

First developed for assaying prohepcidin [17], studies have used ELISA for measuring hepcidin in serum and urine. Lack of information about the physiological properties and importance of prohepcidin in clinical samples makes interpretation of these studies difficult. The main active isoform of hepcidin is believed to be hepcidin-25, but little information is available about how much translated prohepcidin in hepatocytes is released intact. In fact, Valore and Ganz have pointed out recently that most hepcidin released from the cells is the mature 25-residue form produced by furin [13]. Most recently, Ganz *et al.* developed a novel ELISA system for human serum hepcidin and it is expected that this method will be a powerful tool for clinical investigations, but it is unclear whether this method can be applied for *in vitro* research [23].

Methods utilizing MS-based modalities such as SELDI-TOF-MS have been widely used for measuring hepcidin in serum and urine samples [19]. However, the reliability of SELDI-TOF-MS for quantifying multiple molecules such as hepcidin isoforms is still unclear.

We recently developed a method utilizing LC/ESI-MS/MS for quantification of hepcidin [22]. We aimed to improve and extend this method to apply it for measurement of

© 2009 WILEY-VCH Verlag GmbH & Co. KGaA, Weinheim

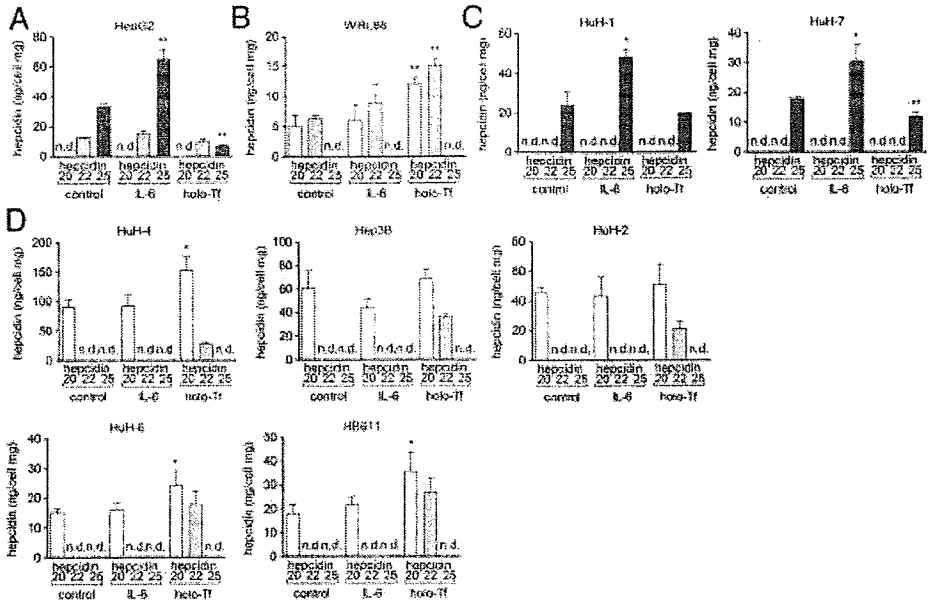

Figure 4. Quantification of hepcidin isoforms in the culture media of hepatoma-derived cell lines. The patterns of the expression of hepcidin isoforms were different among cell lines, and divided into four groups. (A) HepG2 cells, (B) WRL68 cells, (C) HuH-1 and HuH-7 cells, and (D) HB611, Hep3B, HuH-2, HuH-4, and HuH-6 cells. $*p<0.05$, $**p<0.01$, n.d.: not detected.

hepcidin secreted in culture media by hepatoma-derived cell lines. Our present assay, using MS with trichloroacetic acid precipitation, succeeds in this. Moreover, the new method can simultaneously detect and distinguish hepcidin-20, -22, and -25. The linear relationship between the peak area and hepcidin concentration provides simultaneous quantification of hepcidin-20, -22, and -25 isoforms. To our knowledge, this is the first report for simultaneous and quantitative measurement of hepcidin isoforms, applicable to evaluating hepcidin levels and their response to various stimulations for research using cultured cells. We believe that this method can be applied to clinical as well as research studies, thereby providing new information about hepcidin isoforms levels in serum. Determination of hepcidin isoforms may also be a biomarker for differential diagnosis and evaluation of disease activity in clinical studies, although further investigation is needed.

One advantage of our method is that it does not depend upon an antibody against hepcidin. Specificity of antibodies used for quantification of hepcidin requires validation to exclude the possibility that they recognize two or three isoforms of hepcidin simultaneously. Our method can also measure many samples in a relatively short time, so that it is useful for clinical samples and samples from *in vitro* research. However, it does require internal standards of hepcidin isoforms and mass spectrometers but still may be of interest in diverse laboratories.

We found differences in expression of *HAMP* mRNA among cell lines derived from hepatocytes. This finding indicates that such differences must be considered in using these cell lines for research in hepcidin expression.

HLE, HLF, and SK-HEP-1 cells exhibited low *HAMP* mRNA expression in qRT-PCR and did not secrete detectable hepcidin. They may have lost some physiological functions common to hepatocytes.

There were unexpected differences of secretion and response to various stimulations of hepcidin isoforms among cell lines. The cell lines that secreted detectable hepcidin in our study can be divided into at least four groups, suggesting that hepatocytes in the liver *in vivo* might possess different characteristics from each other. We believe this is the first report of the variety of hepcidin isoforms' expression patterns in hepatoma-derived cell lines. Possibly, one subset of hepatocytes is involved in only iron metabolism, while another line is involved in both iron metabolism and the antimicrobial system.

Care should be taken in evaluating hepcidin expression from transcriptional levels because we did not find any obvious correlation between *HAMP* mRNA expression and hepcidin secretion (Figs. 3 and 4). Moreover, different cell lines exhibit different patterns of hepcidin isoforms' secretion. Our data indicate that HuH-7 cells and Hep3B cells each express an mRNA of the *HAMP* gene as determined by RT-PCR. However, HuH-7 cells secrete only hepcidin-25 into the culture medium, and Hep3B cells secrete hepcidin-20 but no detectable hepcidin-25. These observations indicate a risk of misinterpretation if only transcriptional studies are performed for investigation of hepcidin expression, especially for *in vitro* research.

In this study, we subjected HepG2 cells to various stimulations, and observed changes of hepcidin-22 and -25 levels in culture media. The changes of hepcidin-22 and -25 were not parallel; therefore, again the determination of only *HAMP* mRNA might lead to misinterpretation, so simultaneous determination of hepcidin isoforms is strongly recommended. We observed changes of hepcidin-25 that are

© 2009 WILEY-VCH Verlag GmbH & Co. KGaA, Weinheim

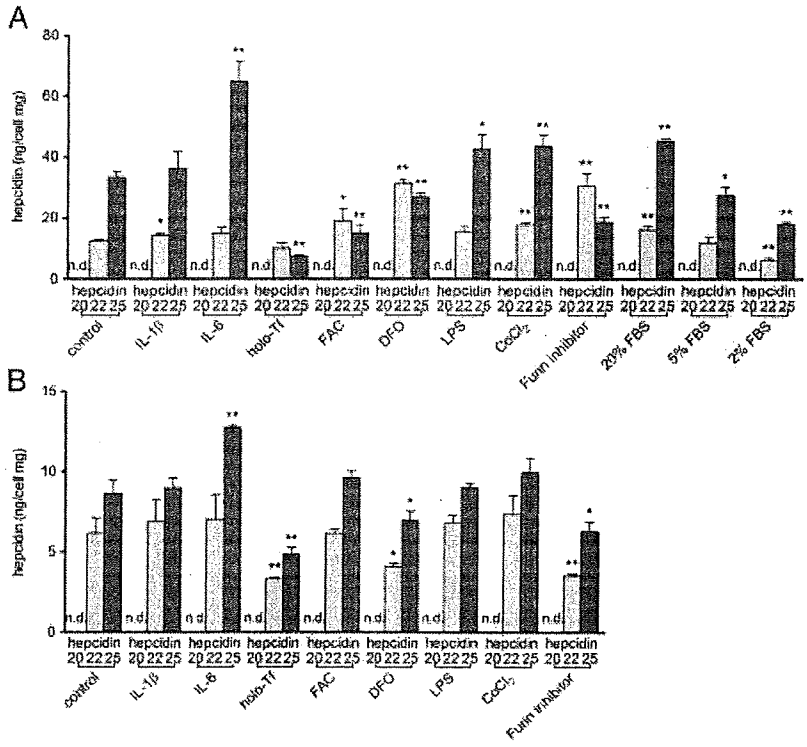

Figure 5. (A) Changes of hepcidin isoforms' expressions induced by various stimulations in the HepG2 cells. IL-6 (20 ng/mL), IL-1β pg/mL, holo-Tf (30 μM), FAC (100 μM), DFO (100 μM), $CoCl_2$ (50 μM), LPS (1 μg/mL), and furin inhibitor (50 μM) were added to the culture media of HepG2 cells as indicated. In addition, the effect of the concentrations of FBS on the expressions of hepcidin isoforms was determined. (B) HepG2 cells were incubated with serum-free medium UltraCulture. Hepcidin expression levels were all lower than those observed in FBS-containing medium. IL-6, IL-1β, holo-Tf, FAC, DFO, $CoCl_2$, LPS and furin inhibitor were also added to observe their effects on hepcidin isoforms' expressions. $^{*}p<0.05$, $^{**}p<0.01$, n.d.: not detected.

consistent with data previously reported elsewhere so that our method for quantification of hepcidin isoforms would be useful for investigating responses of hepatocytes to various stimulations. Observed changes that remain unexplained indicate a need for further investigation of the responses of hepatocytes to various stimulations in their expression of hepcidin isoforms.

We realize that varying concentrations of FBS might lead to different results even in the presence of identical stimulations. For example, the furin inhibitor decreased hepcidin-25 while hepcidin-22 was increased (Fig. 5A) in the presence of FBS. This suggests that the pathway for producing hepcidin-22 was activated when the pathway for producing hepcidin-25 was inhibited by furin inhibitor, thereby maintaining the total concentration of hepcidin although skewing the balance between isoforms. However, the precise mechanism of the effect is not known. Both hepcidin-22 and -25 were suppressed when cells were treated with furin inhibitor in FBS-free conditions (Fig. 5B), and this is contrary to the result observed in the presence of FBS. We speculated that the absence of FBS may stress the cells, increasing the sensitivity to furin inhibitor. We recognize that furin is a proprotein convertase acting on hepcidin expression at the posttranslational level [13], so that its inhibition should not be selectively affected by FBS. It is also possible, however, that unknown factors in FBS might upregulate hepcidin-22, since its concentration in FBS-free conditions could not be increased in our study. It may be advisable, therefore, to provide precisely controlled concentrations of FBS in further studies of expression of hepcidin isoforms *in vitro*, since FBS may already contain stimulants of hepcidin expression.

In conclusion, we have devised a method for simultaneous quantification of hepcidin-20, -22, and -25 in culture media by hepatoma-derived cell lines. Using this method, we determined the expression patterns of hepcidin isoforms and their responses to various stimulations in cultured cells, and we found that there are substantial differences among cell lines. We also found no obvious correlation between *HAMP* mRNA expressions and hepcidin isoforms' secretion. Levels of prohepcidin in the culture medium were too low to be detected by ELISA, indicating the necessity of directly measuring hepcidin instead of estimating it from prohepcidin measured by ELISA, especially *in vitro* studies. We believe that our method can contribute to *in vitro* research on the regulation of hepcidin expression, needed because the regulation of hepcidin expression is complex and difficult to investigate precisely *in vivo*.

The authors thank Dr. Philip Aisen for reviewing this manuscript.

The authors have declared no conflict of interest.

5 References

[1] Andrews, N. C., Forging a field: the golden age of iron biology. *Blood* 2008, *112*, 219–230.

© 2009 WILEY-VCH Verlag GmbH & Co. KGaA, Weinheim

[2] Ganz, T., Hepcidin, a key regulator of iron metabolism and mediator of anemia of inflammation. *Blood* 2003, *102*, 783–788.

[3] Nemeth, E., Tuttle, M. S., Powelson, J., Vaughn, M. B. *et al.*, Hepcidin regulates cellular iron efflux by binding to ferroportin and inducing its internalization. *Science* 2004, *306*, 2090–2093.

[4] Pietrangelo, A., Hemochromatosis: an endocrine liver disease. *Hepatology* 2007, *46*, 1291–1301.

[5] Papanikolaou, G., Samuels, M. E., Ludwig, E. H., MacDonald, M. L. *et al.*, Mutations in HFE2 cause iron overload in chromosome 1q-linked juvenile hemochromatosis. *Nat. Genet.* 2004, *36*, 77–82.

[6] Nemeth, E., Roetto, A., Garozzo, G., Ganz, T., Camaschella, C., Hepcidin is decreased in TFR2 hemochromatosis. *Blood* 2005, *105*, 1803–1806.

[7] Nemeth, E., Rivera, S., Gabayan, V., Keller, C. *et al.*, IL-6 mediates hypoferremia of inflammation by inducing the synthesis of the iron regulatory hormone hepcidin. *J. Clin. Invest.* 2004, *113*, 1271–1276.

[8] Nemeth, E., Valore, E. V., Territo, M., Schiller, G. *et al.*, Hepcidin, a putative mediator of anemia of inflammation, is a type II acute-phase protein. *Blood* 2003, *101*, 2461–2463.

[9] Lee, P., Peng, H., Gelbart, T., Wang, L., Beutler, E., Regulation of hepcidin transcription by interleukin-1 and interleukin-6. *Proc. Natl. Acad. Sci. USA* 2005, *102*, 1906–1910.

[10] Inamura, J., Ikuta, K., Jimbo, J., Shindo, M. *et al.*, Upregulation of hepcidin by interleukin-1beta in human hepatoma cell lines. *Hepatol. Res.* 2005, *33*, 198–205.

[11] Verga Falzacappa, M. V., Vujic Spasic, M., Kessler, R., Stolte, J. *et al.*, STAT3 mediates hepatic hepcidin expression and its inflammatory stimulation. *Blood* 2007, *109*, 353–358.

[12] Babitt, J. L., Huang, F. W., Wrighting, D. M., Xia, Y. *et al.*, Bone morphogenetic protein signaling by hemojuvelin regulates hepcidin expression. *Nat. Genet.* 2006, *38*, 531–539.

[13] Valore, E. V., Ganz, T., Posttranslational processing of hepcidin in human hepatocytes is mediated by the prohormone convertase furin. *Blood Cells Mol. Dis.* 2008, *40*, 132–138.

[14] Kulaksiz, H., Theilig, F., Bachmann, S., Gehrke, S. G. *et al.*, The iron-regulatory peptide hormone hepcidin: expression and cellular localization in the mammalian kidney. *J. Endocrinol.* 2005, *184*, 361–370.

[15] Nemeth, E., Preza, G. C., Jung, C. L., Kaplan, J. *et al.*, The N-terminus of hepcidin is essential for its interaction with ferroportin: structure–function study. *Blood* 2006, *107*, 328–333.

[16] Park, C. H., Valore, E. V., Waring, A. J., Ganz, T., Hepcidin, a urinary antimicrobial peptide synthesized in the liver. *J. Biol. Chem.* 2001, *276*, 7806–7810.

[17] Kulaksiz, H., Gehrke, S. G., Janetzko, A., Rost, D. *et al.*, Pro-hepcidin: expression and cell specific localisation in the liver and its regulation in hereditary haemochromatosis, chronic renal insufficiency, and renal anaemia. *Gut* 2004, *53*, 735–743.

[18] Merle, U., Fein, E., Gehrke, S. G., Stremmel, W., Kulaksiz, H., The iron regulatory peptide hepcidin is expressed in the heart and regulated by hypoxia and inflammation. *Endocrinology* 2007, *148*, 2663–2668.

[19] Tomosugi, N., Kawabata, H., Wakatabe, R., Higuchi, M. *et al.*, Detection of serum hepcidin in renal failure and inflammation by using ProteinChip System. *Blood* 2006, *108*, 1381–1387.

[20] Kartikasari, A. E., Roelofs, R., Schaeps, R. M., Kemna, E. H. *et al.*, Secretion of bioactive hepcidin-25 by liver cells correlates with its gene transcription and points towards synergism between iron and inflammation signaling pathways. *Biochim. Biophys. Acta* 2008, *1784*, 2029–2037.

[21] Murphy, A. T., Witcher, D. R., Luan, P., Wroblewski, V. J., Quantitation of hepcidin from human and mouse serum using liquid chromatography tandem mass spectrometry. *Blood* 2007, *110*, 1048–1054.

[22] Murao, N., Ishigai, M., Yasuno, H., Shimonaka, Y., Aso, Y., Simple and sensitive quantification of bioactive peptides in biological matrices using liquid chromatography/selected reaction monitoring mass spectrometry coupled with trichloroacetic acid clean-up. *Rapid Commun. Mass Spectrom.* 2007, *21*, 4033–4038.

[23] Ganz, T., Olbina, G., Girelli, D., Nemeth, E., Westerman, M., Immunoassay for human serum hepcidin. *Blood* 2008, *112*, 4292–4297.

[24] Lin, L., Valore, E. V., Nemeth, E., Goodnough, J. B. *et al.*, Iron transferrin regulates hepcidin synthesis in primary hepatocyte culture through hemojuvelin and BMP2/4. *Blood* 2007, *110*, 2182–2189.

[25] Nicolas, G., Chauvet, C., Viatte, L., Danan, J. L. *et al.*, The gene encoding the iron regulatory peptide hepcidin is regulated by anemia, hypoxia, and inflammation. *J. Clin. Invest.* 2002, *110*, 1037–1044.

© 2009 WILEY-VCH Verlag GmbH & Co. KGaA, Weinheim

Biochemical and Biophysical Research Communications 382 (2009) 348–352

Contents lists available at ScienceDirect

Biochemical and Biophysical Research Communications

journal homepage: www.elsevier.com/locate/ybbrc

A Jak2 inhibitor, AG490, reverses lipin-1 suppression by TNF-α in 3T3-L1 adipocytes

Yoshihiro Tsuchiya [a], Nobuhiko Takahashi [a,*], Takayuki Yoshizaki [a], Sachie Tanno [a], Masumi Ohhira [a], Wataru Motomura [b], Satoshi Tanno [a], Kaoru Takakusaki [c], Yutaka Kohgo [d], Toshikatsu Okumura [a]

[a] Department of General Medicine, Asahikawa Medical College, 2-1-1-1, Midorigaoka-Higashi, Asahikawa, Hokkaido 078-8510, Japan
[b] Department of Microbiology, Asahikawa Medical College, 2-1-1-1, Midorigaoka-Higashi, Asahikawa, Hokkaido 078-8510, Japan
[c] Department of Physiology, Division of Neural Function, Asahikawa Medical College, 2-1-1-1, Midorigaoka-Higashi, Asahikawa, Hokkaido 078-8510, Japan
[d] Department of Medicine, Division of Gastroenterology and Hematology/Oncology, Asahikawa Medical College, 2-1-1-1, Midorigaoka-Higashi, Asahikawa, Hokkaido 078-8510, Japan

ARTICLE INFO

Article history:
Received 28 February 2009
Available online 10 March 2009

Keywords:
Lipin
Obesity
TNF-α
Jak2
Adipocytes

ABSTRACT

Lipin-1 is a multifunctional metabolic regulator, involving in triacylglycerol and bioactive glycerolipids synthesis as an enzyme, transcriptional regulation as a coactivator, and adipogenesis. In obesity, adipose lipin-1 expression is decreased. Although lipin-1 is implicated in the pathogenesis of obesity, the mechanism is still not clear. Since TNF-α is deeply involved in the pathogenesis of obesity, insulin resistance, and diabetes, here we investigated the role of TNF-α on lipin-1 expression in adipocytes. Quantitative PCR studies showed that TNF-α suppressed both lipin-1A and -1B isoform expression in time- and dose-dependent manners in mature 3T3-L1 adpocytes. A Jak2 inhibitor, AG490, reversed the suppressive effect of TNF-α on both lipin-1A and -1B. In contrast, NF-κB, MAPKs, ceramide, and β-catenin pathway tested were not involved in the mechanism. These results suggest that TNF-α could be involved in obesity-induced lipin-1 suppression in adipocytes and Jak2 may play an important role in the mechanism.
© 2009 Elsevier Inc. All rights reserved.

Introduction

Lipin-1 was identified as a responsive mutant gene in fatty liver dystrophy (*fld*) mouse at the year of 2001 and acts as phosphatidic acid phosphatase-1 which is involving in a synthesis of triacylglycerol [1,2]. The member of mammalian lipin family has been classified into lipin-1A, -1B, -2, and -3 with distinct tissue expression patterns [2,3]. Lipin-1 is predominantly expressed in adipose tissue and skeletal muscle. Transient overexpression of lipin-1A or -1B in mouse embryonic fibroblasts showed that lipin-1A is required for adipogenesis, whereas lipin-1B induces lipogenic genes [3,4]. In liver, lipin-1 is working as a transcriptional coactivator for peroxisome proliferator-activated receptors (PPARs) and PPAR-γ coactivator-1 thereby controlling of hepatic lipid metabolism [5]. Lipin-1 may also act on the assembly and secretion of hepatic very low density lipoproteins [6]. From these findings, lipin-1 should be considered as a multifunctional metabolic regulator instead of a lipid-regulating enzyme (reviewed in [7,8]).

In human studies, Yao-Borengasser et al. [9] showed that the expression level of lipin-1 in subcutaneous white adipose tissue is decreased in patients presenting impaired glucose tolerance and is inversely correlated to the body mass index more strongly in lipin-1B than -1A. Similar studies were reported that the expression level of lipin-1 in subcutaneous white adipose tissue is decreased in obesity or the patients representing metabolic syndrome and the decrease is recovered by weight reduction [10,11]. In contrast, adipocyte specific lipin-1 transgenic mice showed obesity phenotype but strikingly amelioration of insulin resistance [12]. Although these findings suggest that the expression level of adipose lipin-1 contributes to adipocyte functions, little is known about the mechanism of decreased lipin-1 expression in obesity. To elucidate the precise molecular mechanism of attenuated adipose lipin-1 expression in obesity will clue to a therapeutic target for obesity and insulin resistance.

Obesity triggers a chronic inflammatory state and cytokine release from either adipocytes or macrophages infiltrating adipose tissue [13,14]. Since TNF-α is addressed to a key cytokine for altering metabolic function of adipocytes, we made a hypothesis that TNF-α plays a role in decreased adipose lipin-1 expression in obesity. To clarify the above hypothesis, we investigated here a role of TNF-α on lipin-1 mRNA expression in 3T3-L1 adipocytes.

Materials and methods

Chemicals. TNF-α and desipramine hydrochloride were purchased from Sigma (St. Louis, MO). SN50 and C_2-Ceramide were purchased from Biomol (Plymouth Meeting, PA). U0126,

* Corresponding author. Fax: +81 166 68 2846.
E-mail address: ntkhs@asahikawa-med.ac.jp (N. Takahashi).

0006-291X/$ - see front matter © 2009 Elsevier Inc. All rights reserved.
doi:10.1016/j.bbrc.2009.03.021

SB202190, SP600125, GSK-3β inhibitor VIII, and AG490 were purchased from Calbiochem (San Diego, CA) and were dissolved in dimethyl sulfoxide (DMSO) with a final concentration of 0.1% DMSO in culture medium. Bovine serum albumin (BSA) used was free fatty acid-free grade (Sigma).

Cell culture. 3T3-L1 fibroblasts were purchased from the American Type Culture Collection (Manassas, VA) and maintained in Dulbecco's modified Eagle's medium (DMEM, Sigma) with 4.5 g/l glucose supplemented with 10% bovine serum (Invitrogen, Carlsbad, CA). Before adipocytic induction, confluent fibroblasts were cultured to DMEM supplemented with 10% fetal bovine serum (FBS, Invitrogen) for 2 days. Differentiation of 3T3-L1 preadipocytes was induced by exposing the confluent cells to insulin (2 μM), 3-isobutyl-methyl-xanthine (0.5 μM), and dexamethasone (1 μM) for 2 days, and then to insulin (2 μM) alone for an additional 2 days. After incubation with these reagents, the medium containing 10% FBS was replenished every other day. Cells were used 13–14 days after differentiation induction when exhibiting more than 95% adipocytes phenotype. Before exposing TNF-α or each reagent indicated in the text, differentiated adipocytes were serum-starved in serum-free DMEM containing 0.1% BSA for 12 h.

Quantitative real-time reverse transcription-PCR analysis. Total RNA was extracted from 3T3-L1 adipocytes using TRIzol reagent (Invitrogen). Complimentary DNA was synthesized with random primers using High Capacity cDNA Reverse Transcription Kit (Applied Biosystems, Foster City, CA). Quantitative real-time RT-PCR analysis was performed with an Applied Biosystems 7300 Sequence Detection System using TaqMan Gene Expression master mix according to the manufacturer's specifications (Applied Biosystems). Validated TaqMan Gene Expression Assays containing gene specific TaqMan probes and primers for mouse lipin-1A (Assay Identification No. Mm00522205_m1 corresponding to GenBank Accession No. NM_172950), mouse lipin-1B (Mm01276800_m1, NM_015763) were used for assay-on-demand gene expression products (Applied Biosystems). To normalize the relative expression of the genes of interest, the Eukaryotic 18S rRNA (Hs99999901_s1, X03205.1) gene was used as an endogenous control. All experiments were performed at least in triplicate. Amplification data were analyzed by comparative threshold cycles (CT) method with a Sequence Detection Software version 1.4 (Applied Biosystems). The 2-ΔΔCT method was used to calculate the relative mRNA expression [15].

Statistical analysis. Data are expressed as the means ± SE. Statistical analysis was performed by analysis of variance and subsequent Newman–Keuls multiple comparison tests using GraphPad Prism Software Version 4. $P < 0.05$ was considered statistically significant.

Results

First, we made to elucidate whether murine TNF-α suppresses lipin-1 mRNA expression in fully differentiated 3T3-L1 adipocytes. As demonstrated in Fig. 1A–D, TNF-α suppressed both lipin-1A and -1B mRNA expression in dose- and time-dependent manners.

To elucidate a possible mechanism by which TNF-α-induced lipin-1A and -1B gene suppressions, we examined if intracellular TNF-α signaling molecules such as nuclear factor-kappa B (NF-κB), mitogen-activated protein kinases (MAPKs), ceramide, and β-catenin/TCF pathway, may be implicated in the mechanism. To evaluate the effect of NF-κB, SN50, a cell-permeable peptide which inhibits translocation of the NF-κB active complex into nucleus [16], was tested. As illustrated in Fig. 2A and B, SN50 did not reverse the effect of TNF-α on lipin-1 expression. Mitogen-activated protein kinases (MAPKs) are a family of three dis-

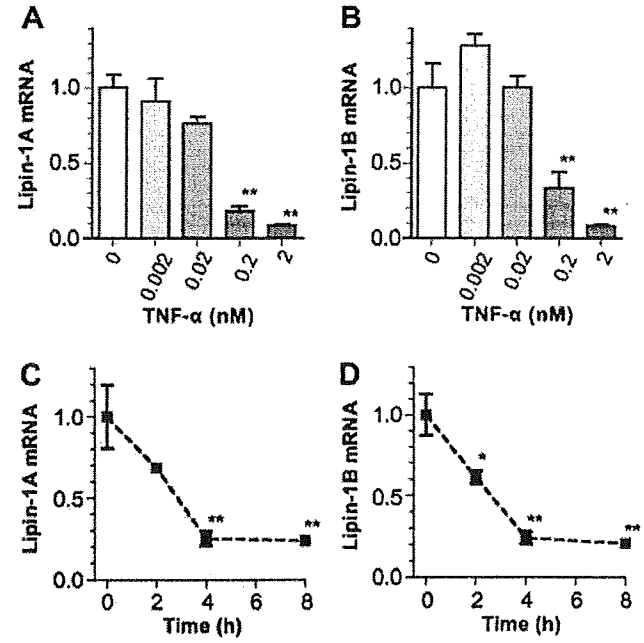

Fig. 1. Effect of TNF-α on mRNA expression of lipin-1A and lipin-1B in 3T3-L1 adipocytes. Serum-starved 3T3-L1 adipocytes (Day 14) were used. Dose-response effects of TNF-α (0.2 nM, 8 h) on lipin-1A and -1B mRNA expression (A,B) and time-course change of lipin-1A and -1B mRNA expression by TNF-α in a dose of 0.2 nM were shown (C,D). The culture medium contained 0.1% DMSO in order to be same condition throughout the experiments. At the end of the treatment, specific mRNA was quantified by real-time RT-PCR. Data are normalized relative to the mRNA levels of 18S rRNA and expressed as the mean ± SE ($n = 3$). $^{*}P < 0.05$, $^{**}P < 0.01$ vs. vehicle alone (A,B) or a group of time 0 (C,D).

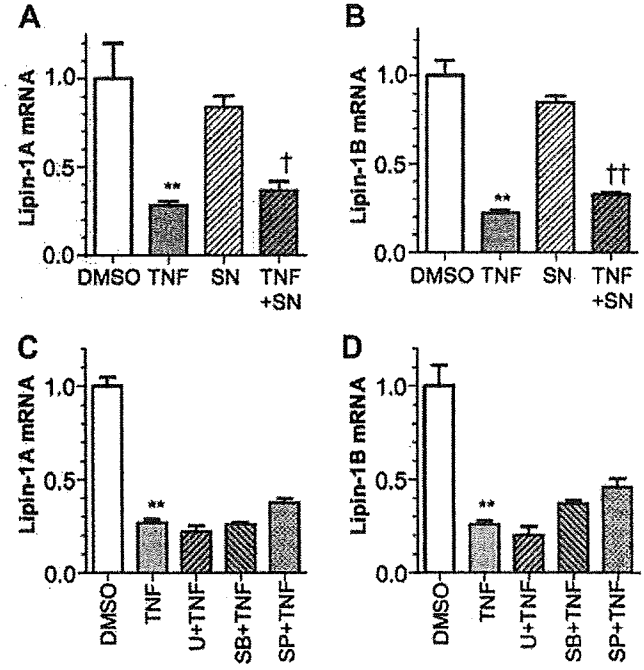

Fig. 2. Effects of NF-kB or MAPK inhibitor on TNF-α-induced lipin-1A and -1B gene suppression. Serum-starved 3T3-L1 adipocytes (Day 14) were cultured in the presence of SN50 (SN, 18 μM) (A,B), U0126 (U, 10 μM), SB202190 (SB, 10 μM), or SP600125 (SP, 20 μM) (C,D) for 1 h before TNF-α (TNF, 0.2 nM, 8 h) was added. At the end of the treatment, specific mRNA was quantified. Data are calculated by fold change vs. DMSO control and expressed as the mean ± SE ($n = 3$–4). $^{**}P < 0.01$ vs. DMSO; $^{\dagger}P < 0.05$, $^{\dagger\dagger}P < 0.01$ vs. SN alone.

tinct protein kinases termed MEK-ERK1/2, p38, and c-Jun N-terminal kinase (JNK) and involving in the intracellular signaling of TNF-α. To clarify whether each MAPK signaling is involved in the reduced expression of lipin-1 mRNA by TNF-α, we examined the effects of each kinase inhibitor for MEK (U0126), p38 (SB202190), or JNK (SP600125) on the inhibition of mRNA expression of lipin-1 by TNF-α in 3T3-L1 adipocytes. As demonstrated in Fig. 2C and D, pretreatment with each MAPK inhibitor failed to block the suppression of lipin-1A and -1B mRNA by TNF-α.

To examine a role of ceramide signaling, the cells were exposed to C_2-Ceramide, a cell-permeable ceramide analog, at a concentration of 50 or 100 μM for 8 h. C_2-Ceramide did not affect on both the lipin-1A and -1B mRNA expression (Fig. 3A and B). Because ceramide is synthesized from sphingomyelin by sphingomyelinase, we additionally examined the effect of desipramine, a sphingomyelinase inhibitor, on the reduced expression of lipin-1 mRNA by TNF-α. As shown in Fig. 3C and D, TNF-α significantly inhibited mRNA expression of lipin-1A and -1B in 3T3-L1 adipocytes that had been pretreated with desipramine. To test the involvement of a β-catenin/TCF pathway in the TNF-α-induced lipin-1 suppression, we used an inhibitor for glycogen synthase kinase-3β (GSK-3β), which inhibits β-catenin by phosphorylation and degradation. Fig. 3E and F showed that GSK-3β inhibitor VIII did not affect on both the lipin-1A and -1B gene expression either in the absence or presence of TNF-α.

Since TNF-α induces the tyrosine phosphorylation and activation of the intracellular Janus tyrosine kinase-2 (Jak2) in 3T3-L1 adipocytes [17], we next investigated whether Jak2 could be involved in the suppressive effect on lipin-1 expression by TNF-α. As seen in Fig. 4A and B, AG490 (50 μM), a Jak2 inhibitor [18], completely blocked the reduced expression of lipin-1A, while partly blocked that of lipin-1B.

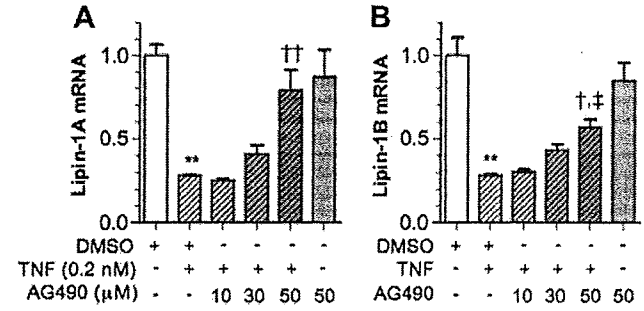

Fig. 4. Effects of AG490, a Jak2 inhibitor, on TNF-α-induced lipin-1A and -1B gene suppression. Serum-starved 3T3-L1 adipocytes (Day 14) were cultured in the presence or absence of AG490 (10–50 μM) for 1 h before TNF-α (TNF, 0.2 nM, 8 h) was added. At the end of the treatment, specific mRNA was quantified (A,B). Data are calculated by fold change vs. DMSO control and expressed as the mean ± SE ($n = 3$–4). Similar results were obtained from three independent experiments. $^{**}P < 0.01$ vs. DMSO; $^{\dagger}P < 0.05$, $^{\dagger\dagger}P < 0.01$ vs. TNF-α alone; $^{\ddagger}P < 0.05$ vs. AG490 (50 μM) alone.

Discussion

Lipid-regulating enzymes often affect whole body metabolism in addition to lipid metabolism. For examples, acyl CoA:diacylglycerol acyltransferase 1 or mitochondrial acyl-CoA:glycerol-*sn*-3-phosphate acyltransferase 1 knockout mice exhibited increased insulin sensitivity [19,20]. Moreover, we have recently reported that diacylglycerol kinase might be involved the glucose transport in muscle cells [21]. Here we focused on lipin-1, one of lipid-regulating enzymes, which works as phosphatidic acid phosphatase-1 to convert phosphatidic acid into diacylglycerol [2]. In obesity, adipose lipin-1 expression is decreased in agreement with several reports [9–11]. In contrast, adipose specific overexpression of lipin-1

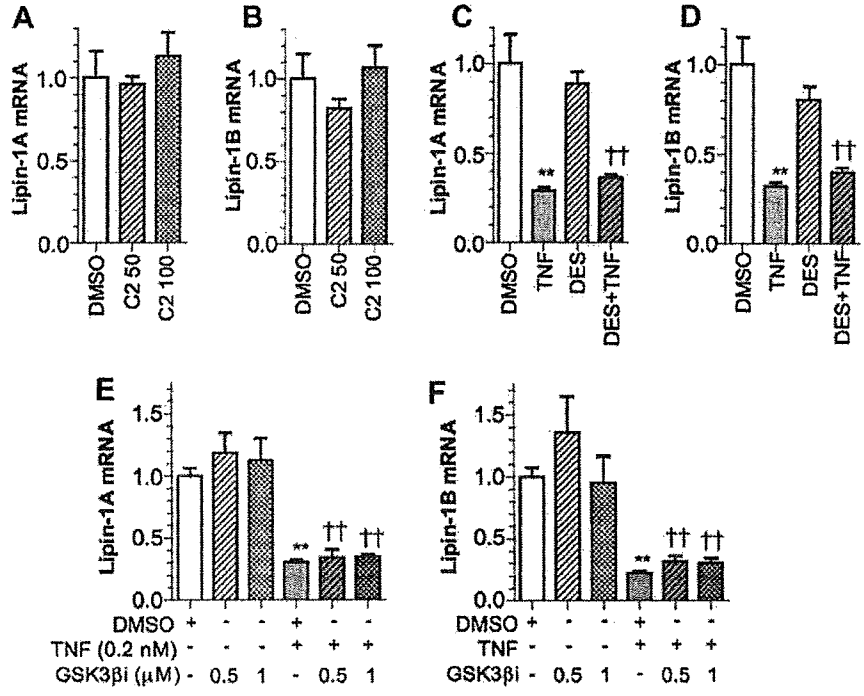

Fig. 3. Effects of ceramide signaling and GSK-3β inhibitor on TNF-α-induced lipin-1A and -1B gene suppression. Serum-starved 3T3-L1 adipocytes (Day 14) were used. For evaluating ceramide signaling, cells were treated in the presence of C_2-Ceramide (C2, 50 or 100 μM) for 8 h (A,B) or desipramine (DES, 20 μM) for 1 h before TNF-α (TNF, 0.2 nM, 8 h) was added (C,D). In another sets, cells were cultured in the presence of GSK-3β inhibitor VIII (GSK-3β i, 0.5 or 1 μM) for 1 h before TNF-α (TNF, 0.2 nM, 8 h) was added (E,F). At the end of the treatment, specific mRNA was quantified. Data are calculated by fold change vs. DMSO control and expressed as the mean ± SE ($n = 3$–4). $^{**}P < 0.01$ vs. DMSO; $^{\dagger\dagger}P < 0.01$ vs. each vehicle.